

APR 2 1960

WEAPONS EFFECTS FOR PROTECTIVE DESIGN\*

Harold L. Brode  
Physics Division  
The RAND Corporation

P-1951

March 31, 1960

\*Space Technology Laboratories Colloquium,  
El Segundo, March 31, 1960; also UCLA  
Extension Course on Ground Support Systems  
for Missiles and Space Vehicles, 25-30  
April 1960.

Reproduced by

The RAND Corporation • Santa Monica • California

The views expressed in this paper are not necessarily those of the Corporation

## **DISCLAIMER**

**This report was prepared as an account of work sponsored by an agency of the United States Government. Neither the United States Government nor any agency Thereof, nor any of their employees, makes any warranty, express or implied, or assumes any legal liability or responsibility for the accuracy, completeness, or usefulness of any information, apparatus, product, or process disclosed, or represents that its use would not infringe privately owned rights. Reference herein to any specific commercial product, process, or service by trade name, trademark, manufacturer, or otherwise does not necessarily constitute or imply its endorsement, recommendation, or favoring by the United States Government or any agency thereof. The views and opinions of authors expressed herein do not necessarily state or reflect those of the United States Government or any agency thereof.**

## **DISCLAIMER**

**Portions of this document may be illegible in electronic image products. Images are produced from the best available original document.**

SUMMARY

Large yield weapons used against hardened installations create an environment of air and ground shock and of thermal and nuclear radiations in extremes which military systems designers have only recently been obliged to consider. As the hardening requirements rise, and systems are designed to survive closer-in, the explosion phenomena of significance become those associated with a region of intensities of effects beyond our experience and best understanding. These close-in phenomena are examined in this paper with a view to delineating their influence on the survivability of structures and equipment at very high overpressure levels. No specific military system or components are considered. The primary purpose of this paper is to build a general appreciation for the nature of the violent forces with which protective designs must cope.

This presentation of the phenomenology, however, may also be useful in framing design characteristics for hardened systems.

CONTENTS

SUMMARY . . . . .	11
Section	
I. INTRODUCTION . . . . .	1
II. NUCLEAR RADIATION . . . . .	3
III. FIREBALL FORMATION . . . . .	10
IV. THERMAL RADIATION . . . . .	13
V. AIR BLAST . . . . .	17
VI. CRATERING . . . . .	21
VII. GROUND SHOCK . . . . .	25
VIII. AFTER EFFECTS . . . . .	33
 BIBLIOGRAPHY - NUCLEAR RADIATION . . . . .	64
BIBLIOGRAPHY - AIR BLAST AND FIREBALL . . . . .	65
BIBLIOGRAPHY - Ground Shock . . . . .	66

## I. INTRODUCTION

Modern weapon systems invariably begin and end with concern for the effects of nuclear explosions. The final sting in nearly every current or proposed system is a nuclear weapon, and the amount of damage and destruction it is capable of inflicting on an enemy target is of obvious concern to the system planners. But at the outset the vulnerability of a system to nuclear explosions dictates its ability to survive counter-force action. Airplanes in the air, missiles on the ground or in space, and all their necessary support equipment (with which this course is primarily concerned) will be evaluated not only from the standpoint of their reliability in normal operation, but equally importantly in the light of their possible failure in the hostile environment of nuclear explosions. It follows that many components of future military systems will be designed with an eye to survival at close distances from large yield explosions, and that sensible and economic design will be predicated on a knowledge of the nature of the various effects to be experienced in such extreme circumstances. Since it is much easier to harden small items than to harden whole complexes, and since hardening will be costly in every case, hardening will generally be restricted to such components as are essential to the final phases of launching.

To understand better what difficulties can be expected in providing for the continued operation of essential ground support equipment during heavy nuclear attack, one needs a sharp descriptive picture of the nature of a nuclear explosion, and one also requires estimates of the damaging effects and of the level of protection necessary. This lecture aims to

provide a general background in weapons effects. The following sections will cover some specific areas of nuclear explosion phenomena pertinent to the design of hardened systems. These subjects may be identified as follows:

nuclear radiation and shielding  
fireball growth and effects  
thermal radiation  
air blast  
cratering and throwout  
ground shock and effects  
cloud rise and fallout  
afterwinds, dust and debris

Although most of these phenomena are distinct and separate in their effects, they are very closely interrelated and have continuous interactions one upon the other.

### III. NUCLEAR RADIATION

To appreciate the effects of nuclear radiation and the necessary steps for protection we must know (1) the possible effects such radiation may have on humans and on equipment, (2) the expected level of exposure from a nuclear burst, and (3) the efficiency of various shielding materials. Of the various measures of nuclear radiation intensity the roentgen unit for gamma-rays and the "rad" for neutrons will be used here. The roentgen represents an intensity of gamma rays such that 87 ergs is absorbed in one gram of air, but in soft tissue (meat) the same intensity deposits about 97 erg/gm. The rad is defined as the amount of radiation (neutrons) which will produce 100 ergs of absorbed energy per gram of soft tissue. Although the response of biological systems is not directly proportional to the energy absorbed, the neutron dose in terms of rads will serve as a rough measure of allowable human doses. Doses of more than 450 roentgens or rads may be expected to kill 50 per cent of those exposed, and a dose upwards of 700 r will cause 100 per cent fatalities. But a dose of less than 100 r is not expected to cause noticeable degradation of human activity and is not likely to be lethal. Consequently, in areas where personnel will operate during attack, the dose should not be allowed to rise above about 100 rad or roentgens.

The electronic systems must also be protected from intense radiation. Circuits involving semiconductors are particularly sensitive. In general, the level of allowable radiation is fairly sensitive to details of the circuitry. One can state a broad rule for currently typical systems to the effect that for silicon elements the neutron exposure should be kept to less than  $10^{11} n/cm^2$ , and for germanium elements to less than

$10^{12}$  n/cm<sup>2</sup>. Usually diode applications are less sensitive than higher modes of operation, and thin transistors are less sensitive than thick elements. With special attention to circuit design, both the above thresholds for permanent damage might be increased by a power of 10. Other than electronic systems, the only structural materials exhibiting particular sensitivity to radiation are synthetics such as Teflon, which may be damaged by exposure to more than  $10^5$  rad (gamma-rays).

In the above, mention is made of both neutrons per square cm and rads. For typical neutron spectra from nuclear explosions, these measures may be approximately related by the following conversion:

$$\text{one rad} \sim 4.4 \times 10^8 \text{ n/cm}^2.$$

Although the initial nuclear reactions (which are in a way responsible for all the features of a nuclear explosion) take place inside the bomb and are over in a fraction of a microsecond, nuclear radiations persist for long periods after the burst and are scattered or radiated from atoms far outside as well as inside the bomb debris. Approximately 90 per cent of the neutrons generated are absorbed within the bomb, but the remaining fraction which escapes creates impressive doses in the air. An even larger percentage of the gamma-rays emitted during the fission process are absorbed in the bomb, but gamma rays coming from the excited fission fragment nuclei continue to radiate for long times. A further source of gamma-rays results from neutron captures in nitrogen which lead to the emission of gamma-rays about 6 per cent of the time.

Since a bomb may be viewed as a source of a fixed number of neutrons the total neutron flux as a function of the distance from the explosion can be expected to fall off as the inverse square of the distance

corresponding to the increasing area of spherical surfaces at larger radii. In addition, the flux will be reduced by the removal of neutrons absorbed in the air along the way, which leads to an exponential-type decay of the flux.

$$N = \frac{2 \times 10^{22} W_{MT}}{R_{ft}^2} e^{-\frac{Rp}{780}} \text{ n/cm}^2,$$

where  $\rho$  is the density of air in grams per liter ( $\sim 1.1$  for average conditions). In this expression it can be seen that the neutrons per square cm increase in proportion to the yield (which is only approximately true and depends sensitively on the particular weapon) and decreases not only with the inverse square of the distance but by an additional exponential decay. Using the conversion to rads, this formula becomes

$$N = \frac{5 \times 10^{13} W_{MT}}{R_{ft}^2} e^{-\frac{Rp}{780}} \text{ rad.}$$

The source of gamma rays, being dependent on neutron captures and on fission fragment decays, is both a complicated function of time and space. The fission fragment radiation decreases with time about proportional to the inverse 1.2 power of the time, while the capture gammas are nearly all generated in the first 1/100 of a second. Although the gamma-rays traverse the air with roughly the same kind of geometric decrease and absorption behavior as the neutrons, the relatively long time for their emission allows the shock movement of the absorbing air to influence the dosage at distant points. This hydrodynamic effect can cause large increases in the gamma-ray dose over that dose which could be expected in

the absence of the expanding shock wave. But the effect cannot be important at the most close-in distances where very little absorbing air lies between source and receiver even before the blast. Neither can the effect amount to much at very large distances where the air motions are both negligible and late. But at the intermediate ranges, where many mean-free-paths of air stand in between, and where the shock motions are impressive, the hydrodynamic effect must be included in any analysis which aims to predict (even approximately) the levels of radiation.

Since the shock wave is nearly symmetric about the bomb, it does not influence the spherical character of the gamma-ray flux, but it does change the character of the absorption and scattering (Fig. 1). In a formulation similar to that describing the neutron flux, the hydrodynamic effect can be roughly included by allowing the mean-free-path ( $\lambda$ ) and the effective amplitude of the source ( $\alpha$ ) to be functions of the yield:

$$D_\gamma = \frac{3 \times 10^{13} W_{MT}}{R_{ft}^2} \alpha e^{-\frac{\rho R}{\lambda}} \text{ roentgen}$$

$$\alpha \approx 1 + .005 W_{MT}^2$$

$$\lambda = 1300 + 30W + 3W^2 \text{ ft}$$

$$.1 < W_{MT} < 20$$

Properly, the dose is a more complex function of both the yield and the range, but over a limited span of yields and for radii corresponding to a few thousand feet, the above formula may suffice.

As an example of the relative neutron and gamma-ray doses, the approximate dose at half-mile intervals from a one-megaton burst are

listed in Table 1 together with the approximate overpressure to be expected at those distances. Note that the neutron dose is dominant only at the closest station. Such a cross-over between neutron dominance and gamma-ray dose dominance is to be expected, since the source strength is greater for neutrons, but so also is their decay rate.

Table 1

## DOSE VS DISTANCE - ONE MT

Gamma	Neutron	Distance	Overpressure
~ 40 r	~ .5 rad	2 miles	~ 10 psi
~ 500 r	~ 20 rad	1.5 miles	~ 20 psi
~ 10,000 r	~ 1,800 rad	1 mile	~ 40 psi
~ 200,000 r	~ 330,000 rad	.5 mile	~ 200 psi

These numbers reflect the high levels of nuclear radiation present in the air, and in order to reduce the dose to tolerable levels inside protective structures some shielding must be accomplished. What functions shields must perform is obviously related to both the nature and intensity of the radiation and to the sensitivity and location of the equipment or personnel to be sheltered. Some general properties of and requirements for shielding can be set down, however.

Since a shield will ordinarily be required to stop both neutrons and gamma-rays, it should be planned to include materials appropriate to the absorption of each. Gamma-rays are more readily stopped by the heavier elements, the most common such element being lead, but iron is also quite efficient. A rough idea what effect various common shielding materials have on the fission fragment gamma-rays can be seen from the thicknesses required to reduce the flux by 50 per cent. To this effect, it takes six

inches of concrete or eight of earth or twenty-four of wood while only one and one-half of steel will do, and a mere half-inch of lead would reduce the prompt gamma dose to half its initial value (Fig. 2).

Shielding for neutron fluxes is not entirely a simple matter of interposing dense materials, since the neutrons, as uncharged particles, can move through heavy atoms like a golf ball driven through a pile of bowling balls. But, by the same analogy, a golf ball hitting a bucket of golf balls loses its energy much more rapidly. On each collision of a golf ball with a bowling ball, their total momentum is unchanged, i.e. is conserved. In doing this, the massive bowling ball need acquire very little of the golf ball's velocity and hence receive very little kinetic energy from the golf ball to still conserve momentum in their collision. On the other hand, a golf ball striking another golf ball results most often in both acquiring half the initial ball's velocity, thus on each collision the incident ball loses about half its energy.

In an analogous way a neutron may pass through heavy-element material with little loss in energy, while a neutron in hydrogenous material or matter composed largely of light atomic elements, such as water or plastic or other hydrocarbons, may be slowed down to essentially thermal energies and then may be more likely captured in some nucleus. Shields for energetic neutrons, then, are best designed with light element components. But, in some neutron captures very energetic gamma-rays are emitted, so that, for proper shielding from these, more heavy element material may be included. A reasonable compromise is often possible with reinforced concrete or special concrete mixtures with iron punchings or with boron salts added. For more exotic designs, laminates of lead and plastics or parafin or

water are used. Some materials produce radioactive isotopes upon absorbing neutrons, so care should be exercised to avoid those elements that have radioactive half-lives long enough to cause continued danger. It is well to note that the first few inches of shield may reduce the neutron flux more than succeeding inches, since the first inches screen out many low energy neutrons (as well as fast ones), leaving only fast ones for succeeding inches of the shield. Except in the first few inches, where the effectiveness of the shield is even greater, it takes about ten inches of concrete to reduce the flux by a factor of ten, or about twenty inches to cut it by a factor of 100. Special heavy concrete may be as effective in thinner layers, seven inches being roughly equivalent to ten inches of normal concrete. The use of colemanite or other boron salts in the mix can result in even greater absorption ability, since one of the natural isotopes of boron has an unusual affinity for the slow neutrons.

For many but not all situations, the necessary earth cover or concrete and steel for blast protection is more than a sufficient radiation shield.

### III. FIREBALL FORMATION

In an explosion of something like a one-megaton bomb there is a release of energy equivalent to  $10^{15}$  calories in a time much less than a millionth of a second and in a mass of a very few tons. Such a high energy density leads to temperatures of millions of degrees, and leaves much of the energy in the form of radiation. This radiation quite quickly diffuses out of the bomb and into the air. Unlike ordinary visible light, the radiation from the bomb materials at such high temperatures is mostly in the form of X-rays and ultraviolet light and "light" of these high frequencies does not go to large distances in air. Rather, it is absorbed in the air immediately around the bomb, causing that air to be heated to temperatures in the neighborhood of a million degrees centigrade. But air at a million degrees becomes quite transparent even to X-rays and ultraviolet light, so that subsequent radiation from the bomb can traverse this region of hot air more freely and will suffer less absorption. By such a process, then, this initial region of hot air continues to grow as energy pours out of the bomb, and, since the cold air is still quite opaque, a rather sharp front is maintained between the cold air outside and the hot air inside.

The initial growth of this isothermal sphere is much faster than hydrodynamic shocks can move, even at these exalted temperatures. But, as the energy expands by this radiation diffusion process into larger and larger volumes of air and its temperature drops, the speed of the expansion decreases, until, at about  $300,000^{\circ}\text{C}$ , the rate is comparable to a shock speed at the same temperature. After that, an extremely

strong spherical shock wave develops and races onward at unbelievably high Mach number. For a 1 megaton burst, this transition should occur at a radius of about 130 ft from the bomb. The extremely strong shock, driven by the high pressures in this hot sphere, begins to compress the air some ten-fold above normal air density and to force this hot air outward close behind the shock front. Since the shock is expanding into continuously larger volumes of air, its strength, and, consequently, its ability to heat the air it engulfs, decreases rapidly with increasing shock radius. Although the shock-heated air is initially at temperatures well below the interior temperatures, it is hot enough to be intensely luminous (with intensities many times that of the sun). This shock front is the source of the early thermal radiation. As this shock decreases in strength, its luminosity decreases so rapidly that the total radiation from the fireball also decreases in spite of the increasing area of the expanding shock front.

Figure 3 illustrates the early temperature history of this blast wave, showing the temperature in degrees on the Kelvin scale (the absolute centigrade scale) for a one megaton surface burst. The earliest curve (.075 ms) is characteristic of the nearly isothermal fireball formed by the radiation diffusion. At later times the shocked air beyond the isothermal sphere (which is expanding) shows as a region of lower temperature. As the shock decreases in strength, it heats the air less, so that the air behind the shock is hotter than that just at the shock, and a steep increasing gradient in temperature exists from the shock front back to the nearly uniform hot interior.

Since the radiation diffusion growth is initially too fast to induce appreciable motions in air, the air is left at essentially normal air density while its temperature and pressure are raised to values like a million degrees Kelvin and a million psi. As the radiation wave slows in its growth and the high pressures begin to build a strong shock, the air in the hot interior begins to expand to lower densities and the shock thus formed compresses the air ahead to many times normal air density (Fig. 4). The interior of the fireball rapidly becomes evacuated, so that by the time the shock has decreased to a peak pressure of 1000 psi (~ 74 ms and 1500' for 1 MT) the interior density is about one-hundredth of normal air density.

The pressure profiles at these early fireball times are shown in Fig. 5. The earliest air overpressures are indeed like a million pounds per square inch, but rapidly drop as the fireball grows, so that a peak overpressure of 100,000 psi occurs at about 350 ft (for 1 MT) and an overpressure of 10,000 psi occurs at about twice that distance ~ at 700 ft. As a little more than double the distance again, at about 1,500 ft, the peak overpressure is down to 1000 psi.

#### IV. THERMAL RADIATION

Figure 6 shows temperature profiles at late fireball times (as indicated) for the same one megaton surface burst. This is an appropriate point at which to digress from the blast history to discuss the nature of the thermal radiation. As was mentioned, most of the earliest light from the bomb cannot go far in air, but as a shock develops, and the surface of the fireball becomes a sharp shock front, it begins to radiate strongly in the visible at an intensity characteristic of a blackbody at the shock temperature. At times earlier than times illustrated here, only a fraction of the blackbody rate (which is proportional to the fourth power of the temperature) is in the visible spectrum, and only that fraction which is in wave lengths in the visible or infrared can go to large distances. The power or rate of thermal radiation at the earlier times, then, can be expressed as proportional to the surface area of the fireball ( $2\pi R_s^2$ ) times the specific blackbody radiation rate at the shock temperature  $\sigma T_s^4$ , but modified by a factor indicating the fraction of the spectrum that can pass through cold air  $f(T_s)$ .

$$P = 2\pi R_s^2 \sigma T_s^4 f(T_s)$$

At times as late as shown in Fig. 6, the shock front itself is becoming so cool that it is no longer strongly luminous, and the hotter air behind begins to shine through it. Since the hot interior is still expanding and since the radiation intensity increases rapidly with increasing effective temperature, the thermal power rises rather sharply at this time. As the rate of radiation increases, it represents a rapid heat loss which depletes the store of energy in the fireball, and, as

the temperature drops the thermal power again decreases. The depletion and cooling is less rapid, so that the thermal intensity trails off over a period of ten or more seconds. This sequence of optical-hydrodynamic events results in a first fast maximum in the thermal radiation followed by a minimum at around a tenth of a second and by a second maximum at around one second. Since both the time duration of the first maximum is short and the size of the fireball is small, less than half of one per cent of the bomb's energy is radiated before the minimum in the power pulse. The second pulse is longer and radiates from a larger effective surface, so that it emits nearly one-third of the total yield. The main pulse of thermal radiation reaches a maximum in about one second (for the one megaton case) and, as mentioned, lasts about ten seconds. Such huge amounts of energy radiated in such a relatively short time will result in impressive heat loads on any exposed surfaces. Light weight, thin, dry, flammable materials may be ignited by this heat load out to very large distances. Energies from five to fifty calories may be required, however, and thicker, denser or damper materials may only char on the surface without igniting to sustained burning. Under the most "favorable" conditions, such fires could be started at distances as large as ten miles from a one megaton explosion. Degrading factors such as attenuating or scattering clouds, smoke, haze, fog or dust or chance shielding by intervening topography, structures or natural growth must be considered for large yield surface burst effects. For the large yield explosions, the pulse occurs over a sufficiently long period of time for exposed surfaces to char and smoke but in so doing to create partial shields against the bulk of the impinging thermal energy. They thus experience less thermal

damage than could be expected from the total heat inputs. In all of our Pacific tests, there has been no instance (to the author's knowledge) where fires were started at distances beyond those for serious blast damage.

At the very close-in positions of hardened installations the thermal phenomenon is more one of an intensely hot bath in the fireball gases than one of incident thermal radiation. Figure 7 illustrates the time history of the air temperature at some high peak overpressure levels. At 40 psi one is outside the fireball's maximum radius, so that as the shock strikes, the air is raised about  $150^{\circ}\text{C}$  but is then cooled within a couple of seconds to nearly normal air temperature again. The 100 psi station is on the edge of the fireball, and so the temperature continues to rise somewhat after shock arrival. The shock, being stronger here, heats the air to a higher temperature initially (about  $400^{\circ}\text{C}$ ). The air behind the shock is still expanding, but since that air was shocked to even higher temperatures, it exposes the 100 psi point to higher and higher temperatures until the expansion stops. The air flow reverses and eventually ends in the general rising away of the hot remaining fireball.

The 200 psi point is well inside the maximum fireball radius, and the temperature rise after shock arrival indicates that much hotter air engulfs this station. Here the temperature rises from a shock value of  $1000^{\circ}\text{K}$  ( $\sim 700^{\circ}\text{C}$ ) to about  $4000^{\circ}\text{K}$  in less than a second.

Since the fireball is like a bubble in the atmosphere, it begins to rise and so pulls away from the earth's surface in just a few seconds. Using a very approximate model for the effect of this fireball rise on the temperature history at the distance corresponding to a peak overpressure

of 200 psi, it appears that the hot temperatures of the fireball interior will be reduced at this ground range in about the manner indicated by the decreasing tail on the 200 psi curve of Fig. 7. Thus a decrease begins after four or five seconds of exposure, and in fifteen to twenty seconds the air temperature has returned to normal. The other high temperature curves would be similarly reduced at late times by the same effect.

At the 400 psi and the 1000 psi levels the temperatures rise to even higher levels, but subsequently show a more rapid drop (at times less than one second) due to the thermal radiation loss which becomes significant even before the fireball has begun to rise. Even at these high levels one need not expect serious thermal damage to protective structures, since the duration of the heating is too short for serious heat conduction beyond the surface layers of exposed materials. Some pitting and charring, even some evaporation or blow-off on steel or concrete can occur, but reinforced concrete doors mounted flush with the ground surface at 1000 psi from a megaton explosion should not suffer real damage. Elements exposed above ground level may suffer more thermal damage, but most such structures will also be more sensitive to blast damage.

Designs must work to avoid damage to door seals or to interiors through contact with the hot fireball gases. Ingestion by ventilating systems and other openings must be prevented, but the major design problems do not hinge on the temperature or thermal radiation effects that characterize the fireball. There are some even less desirable features than this heat to existence in the inhospitable environment of the fireball interior.

## V. AIR BLAST

Returning to the history of the blast, one finds in Fig. 8 the overpressure profiles extended to later times, larger distances and lower overpressure levels. If one notices the nature of these profiles at the earlier times (before one second), the pressure-time relations (to be discussed next) may be more easily understood. Note that the pressure drops rapidly just behind the shock as one goes to smaller radii, while in the interior there are essentially no pressure gradients. The interior is the very hot region of the fireball where pressure pulses of any sort are transmitted outward very rapidly because of the accompanying high sound speeds at these high temperatures. Near the front, however, the observed positive pressure gradient (as a function of radius) is a necessary feature of the spherically expanding shock, in which the interior gas is constantly decelerated as the shock runs into more and more stationary air.

Because the pressures are so uniform inside the shock and because the pressure rises and falls so sharply at the shock front, the time history of the overpressure at any point is characterized by a bimodal decay (Fig. 9). Immediately after shock arrival the decay is dominated by the passage of the pressure spike associated with the shock front itself. Then, shortly afterwards, the decay is dictated by the general rate of pressure decrease in the more uniform interior, which has by then expanded over the position in question. This time history can be quite well described at all pressure levels by the sum of two decreasing exponential functions, representing the two decay rates.

$$\Delta P = \Delta P_s (ae^{-\alpha t} + be^{-\beta t})(1 - 5/D^+)$$

In order to force this fit to go to zero overpressure at the end of the positive phase, a linear factor has been included which becomes zero at a time equal to the duration of the positive phase, ( $D^+$ ) where the time is measured as the time after shock arrival.

Figure 10 displays the positions of the shock front from a one megaton surface burst illustrating very generally the relative position of the fireball and crater. The rapid increase of peak overpressure as one moves closer to the burst point is strikingly evident. Note that 100 psi occurs just at the edge of the fireball. The high transient winds or air velocities accompanying the shock emphasize the importance of placing protective structures below or at least flush with the surface. The short solid lines below the ground indicate schematically an expected reduction of peak overpressure at depths. The dashed lines are intended to indicate generally the relations between the air shock position and the wave front in the soil at corresponding times. At the higher overpressures (down to 200 or 300 psi) the air shock speed is faster than the seismic velocity of the soil, so that the compression wave in the soil lags behind and propagates downward from the surface along a shallow saucer-shaped wave front. As the air shock speed continues to decrease, at some point it drops below seismic speeds, thus allowing waves in the soil to move out ahead of the air blast. This feature leads to some complication in the ground shock interpretation, and will be touched on again in discussing the ground shock problems.

Some general features of the blast wave are illustrated as a function of the peak overpressure in Fig. 11. Independent of weapon yield, the shock temperature, peak dynamic pressure, shock velocity and maximum

particle velocity at any point are related to the peak overpressure at that point as shown in Fig. 11. The temperature and velocities increase with increasing peak overpressure, but less rapidly than the peak overpressure itself. The peak dynamic or wind pressure rises very rapidly, however, increasing more like the square of the peak overpressure at low overpressures and becoming proportional to the overpressure itself only at the highest levels.

The shock radius and the time of shock arrival depend on the explosion yield, being longer by a factor  $W^{1/3}$  (in MT) for energies greater than a megaton.

The impulse of the blast wave is often a significant parameter in damage prediction. The impulse is the time integral of the pressure taken over the time of the positive phase. Figure 12 shows the general relation of the impulses for overpressure and dynamic pressure (along with the durations of each) to the peak overpressure. From this figure one can determine that the overpressure impulse increases (with increasing overpressure) like the square root of the overpressure below 1000 psi, and about like the cube root at higher overpressures. Since at the higher overpressure levels the overpressure itself is proportional to the inverse cube of the radius, its impulse then is roughly proportional to the inverse radius. The dynamic pressure impulse decreases only very slowly with decreasing overpressure above 100 psi, being proportional in that region to about the fourth root of the overpressure, but it drops from importance exceedingly rapidly at lower overpressures.

Although the total durations of the positive phase of overpressure and air velocity are not changing much with overpressure, as one moves

to higher overpressures the bulk of the impulse is delivered more nearly in the first few milliseconds rather than uniformly over the whole positive phase. As was illustrated in the pressure-time curves, the pulse shapes at high overpressures are much more peaked than at lower overpressures, and the exact duration of the positive phase is less important there than it is at the lowest overpressure levels (where the pulse becomes nearly linear in its time decay).

## VI. CRATERING

The depression left by a megaton bomb exploded on the surface of the ground is quite impressive. The general nature of such nuclear craters is typical of craters from a wide variety of explosive or impact sources. The one MT-surface burst crater (Fig. 13) is relatively shallow, having a diameter which is about nine times its depth. The dimensions, relative shape and zones of rupture and permanent displacement of soil vary widely according to the properties of the earth medium. Hard rock, of course, yields the smallest craters, wet soils the largest, although if the soil is saturated, the crater depth may be quite shallow. For a one megaton surface burst on dry soil, one can expect the volume of the hole to be of the order of 100 million cubic feet, representing the excavation (or compaction) of a few million tons of soil.

The precise height or depth of burst has a very important influence on crater and on the bomb energy delivered into the soil initially. Some consideration of the role of momentum conservation in the initial energy partition between air and ground (for a surface burst) may help explain this sensitivity to depth of burst.

A true contact burst might be expected to deliver half its momentum downward into the soil and half upward into the air. However, only a fraction of the bomb energy finds its way into kinetic motion of the bomb materials. Further, since the soil is at least a thousand times denser than the air, the velocities imparted to the soil are less than those created in the air by just this ratio of the densities, if momentum is to be balanced in accord with Newtonian notions. The kinetic energy

imparted in this way will be proportional to the square of the velocity and so will be much less in the dense material. Actually, something like 15 per cent of a one megaton explosion's energy starts out into the ground.

The extremely high energy densities and temperatures of a nuclear explosion guarantee the validity of a hydrodynamic treatment of the close-in soil response, since the initial strong shock will vaporize the soil for some distance.

Using a two-dimensional hydrodynamic model, and including the effect of the equation of state of one type of soft rock, Robert Bjork, Nancy Brooks and myself at RAND have done some preliminary calculations of such a surface burst. Figure 14 shows the pressure contours as calculated at about one-tenth of a millisecond. Pressures are in kilobars, so that the highest pressures are about seven megabars and are centered in the downward hemispherical shock at about seven meters radius. The presence of the surface has already caused some relief of pressure at shallow depths, but the main shock appears to be fairly uniform and spherically diverging in a vertical cone of about 90° width.

Figure 15 illustrates the velocity field at this same early time, with the same portion of a spherical shock appearing. Rock vapor is already streaming upwards at velocities of several tens of meters per millisecond (or tens of kilometers per second)!

At a time of some fifty milliseconds the pressure contours still show much the same curved shock with continued surface relief (Fig. 16). The shock strength is now down to about seven kilobars at a depth of 160 meters, and pressures are approaching a level where hydrodynamics should give way to considerations for the solid state properties of the

rock--the medium is no longer a true fluid. But carrying the calculation further may lead to reasonable first motion information (i.e., peak velocities and stresses), in spite of the failure of the fluid model to include the elastic properties of a solid. In Fig. 17 the velocity vectors at about 50 milliseconds show the same spherical nature with the high speed jetting above the surface typical of such a burst. Figure 18 shows a continuation of this problem to 100 milliseconds, where the shock pressures are like 3 kilobars at a depth of 250 meters (~ 800 ft). These are pressures of an awkward level to treat: too high for clearly elastic propagation and too low for hydrodynamics to be rigorously applicable in many earth materials. Crushing, plastic and viscoelastic behavior could be expected to have important influences on both the subsequent wave propagation and on the response of an imbedded structure. In this analysis, the portion of the shock running vertically below the burst point remains the strongest, and it may represent a significant limitation to the survivability of structures directly underneath a large yield explosion. It remains to be stated that almost no field experience exists in this regime directly under a crater, although the lack is recognized and is being remedied to some extent.

The corresponding velocity field of this 100 ms time is shown in Fig. 19. A gratifying, if fortuitous, aspect of the velocities at both this time and at the previous 50 ms time is the rather clear division of upward and downward motion by a contour not unlike that which represents the expected final crater profile.

Figure 20 displays the relations between peak pressures (or stresses) versus distance from the point of burst along the vertical (V), the horizontal (H) and along a diagonal at  $45^\circ$  from the vertical (D).

Ignoring the various other curves on this graph, one should note that the early decay of peak pressure follows an inverse cube of the slant distance from the burst point, as expected for a strong shock in any medium. At the lower pressures the decay approaches a more gradual decay--more like the inverse square or inverse three-halves power of the radius. The pressures along the horizontal continue to drop more rapidly even at low stresses since here the rock is in more intimate contact with the much lower air pressures.

Figure 21 offers some idea of the peak velocities as a function of radial distance from the burst point. The maximum velocities occur in the vertical direction and along a vertical line below the burst. The horizontal component of velocity along this same vertical line is very small, indicating mainly the effect of the divergence in the expanding shock wave. The peak velocity components both vertical and horizontal along the surface are as much as a factor of two or three smaller than the maximum velocities along the vertical.

## VII. GROUND SHOCK

Figure 22 should give some feeling for the relative dimensions of the air and ground shocks at about 77 ms, a time when the air shock peak overpressure is 1000 psi. In addition to the intense direct shock in the vicinity of the crater, a ground shock is induced under the air blast slap at the larger distances. As indicated earlier, the air induced portion of the ground shock is initially directed quite vertically since the air blast expands so much faster than the pressure pulse in the ground can travel. Labeling this region as "superseismic," Fred Sauer of Stanford Research Institute has provided the semiempirical and very approximate formulas of Table 2 as guidance in determining the levels of ground shock in this region between the point where the direct or cratering shock ceases to dominate and the distance (or overpressure level) where the air shock speed becomes less than the seismic velocity in the local ground materials.

Table 2  
SUPERSEISMIC GROUND SHOCK

Maxima at 5 ft depth

$(C_L = \text{seismic velocity in rock} = \frac{3}{4} \text{ seismic velocity in soil, ft/sec})$

Vertical acceleration:  $\frac{a_{vm}}{\Delta P_s} = \frac{340}{C_L} \text{ g/psi} \pm 30\%$

$(s = \text{specific gravity - dimensionless})$

Velocity:  $\frac{u_{vm}}{\Delta P_s} = \frac{75}{sC_L} \frac{\text{ft/sec}}{\text{psi}} \pm 20\%$

$(I_p = \text{overpressure impulse in positive phase in psi-sec})$

(Table 2, SUPERSEISMIC GROUND SHOCK continued.)

$$\text{Displacement: } \frac{d_{vm}}{I_p} = \frac{20}{SC_L} (\Delta P_s)^{\frac{1}{4}} \frac{\text{ft}}{\text{psi-sec}} \pm 30\%$$

$$\text{Stress: } \sigma_{vm} = \Delta P_s$$

$$\text{Strain: } \frac{\epsilon_{vm}}{\Delta P_s} = \frac{11 \times 10^4}{SC_L^2} = \frac{\text{PPK}}{\text{psi}} \pm 30\%$$

Note that the vertical acceleration is simply proportional to the peak overpressure of the air shock ( $\Delta P_s$ ) and inversely proportional to the seismic velocity in the medium. For an example, consider a soil with a seismic velocity of 4000 ft/sec (so  $C_L = 3000$ ), then from the information on the air blast (Fig. 11), one can determine that the air shock velocity is faster than this seismic velocity at peak overpressure levels above about 400 psi. If we consider a 500 psi peak overpressure, this formula would give the maximum vertical acceleration as 57 g's, with the uncertainty of 30 per cent allowing the value to be anywhere between 40 and 74 g's.

For the same example, and assuming a specific gravity of two, the peak vertical velocity, according to Sauer's formula, becomes six and one-fourth feet per second, or between five and seven and one-half feet per second.

Since the impulse in the air blast depends on yield, the maximum displacement is a function of both the peak overpressure level and the explosion yield. For a one megaton surface burst, and again at the 500 psi point, the overpressure impulse is about 40 psi-sec, so that for this same soil example the displacement is predicted as between

five and ten inches with a best value being seven and one-half inches.

Although the actual peak stress at depth will depend very much on both the nature of the blast and the nature of the soil, at shallow depths in most media and for large yield explosions it can be assumed to be just the same as the incident peak overpressure. Strain, of course, will depend on the seismic impedance of the material, so that for our example the strain in parts per thousand will be about three, or between two and four.

In order to estimate the ground shock in the more complex region where the ground shocks can outrun the air shock, Sauer has provided the following approximations.

Table 3

GROUND SHOCK OUTRUNNING

$$r = R/W^{1/3}, \text{ kft}/(\text{MT})^{1/3}$$

$$\text{Acceleration: } a_{vm} = \frac{2 \times 10^5}{C_L r^2} g \quad + \text{factor 4} \quad - \text{factor 2}$$

$$\text{Velocity: } u_{vm} = \frac{4 \times 10^5}{SC_L r^2} \text{ ft/sec} \quad + 60 \quad - 40$$

$$\text{Displacement: } \frac{d_{vm}}{W^{1/3}} = \frac{6 \times 10^4}{SC_L r^2} \text{ ft/MT}^{1/3}$$

(reference depth: 10 ft)

To employ the same example of a soil with seismic velocity 4000 ft/sec ( $C_L = 3000$ ) and specific gravity of two for the 100 psi point in a megaton explosion, one must first determine the appropriate radial distance at which one megaton 100 psi occurs (from Fig. 11 it is about

3500 ft), so that the radial parameter in these formulae becomes three and one-half and the maximum acceleration formula gives about five g but with a possible range from two to twenty g equally expected. Such a wide range stems in part from the fact that in this "outrunning" region signals from reflecting or refracting layers in the soil can cause large variations, but also from the fact that the signals from elsewhere in the air blast slap may overlap or pile up as a consequence of the extremely rapid changes in the driving air shock. Figure 23 perhaps overemphasizes the irregular and unpredictable nature of the accelerations in the outrunning phase. Note that some signal arrives prior to the shock arrival directly above the station ( $t = 0$ ). Note also that the maximum acceleration occurs well after shock arrival. One can at least derive some reassurance from the fact that the peak acceleration is less at depth and that some of the sharpness or higher frequency components are missing as one goes deeper. This aspect points to a weakness in the applicability of elastic wave propagation, since any soil or rock must exhibit some energy absorption and nonlinearity. Dissipative mechanisms either natural or artificial can be extremely effective in reducing peak stress or velocity--and a few applications have relied heavily on just such properties.

Following the same example, one finds the maximum velocity for the 100 psi point (but 10 ft down) from a one MT burst lies between three and nine ft/sec, with a mean prediction of five and four-tenths ft/sec. Similarly, the maximum displacement for this case comes out as about 10 inches, but here, as with the rest of these semi-empirical formulae, Sauer has many words of caution for the user. These expressions will surely fail when pushed to regions of overpressure, or yields of weapons,

or types of soil or rock much beyond the realm of our test experience.

The underlying assumption in formulating these scaling rules has been that of elastic response, a fact which cannot be overemphasized since it requires only a little imagination to picture combinations of natural materials and levels of stress which can result in very nonelastic responses.

In designing for shock isolation some information on the frequency characteristics of the ground shock is helpful. At high frequencies (greater than  $\sim 100$  cps), the accelerations are most significant, since neither large amplitudes nor high velocities are likely to occur when the motions are reversing hundreds of times per second. But between 100 cps and about one cps, maximum velocities can become important. At the lowest frequencies the concern is not for velocities or accelerations, which are likely to be quite modest, but for the actual displacements, since at fractions of a cps the amplitudes of oscillations can become a matter of several feet, and isolating or damping mechanisms must provide adequate room to swing without colliding with walls and unmounted equipment.

On this basis, a convenient form in which to express the shock spectra input to a structure is on a harmonic plot which specifies a peak acceleration above 100 cps, a peak velocity between one and 100 cps and a maximum displacement below one cps. A plot combining all of these is roughly possible because of the harmonic nature of elastic wave propagation, and Fig. 24 is such a plot for the vertical ground shock spectra, showing some arbitrary limits for 100 psi and 500 psi for a soil of fairly representative properties. These limits are intentionally on the high side to compensate for some of the uncertainties in the inputs. Figure 25

illustrates similar estimates for the horizontal ground shock motions. Comparison with the vertical spectra of Fig. 24 will show that although maximum expected accelerations are about the same, peak velocities and maximum displacements are estimated to be much less in the horizontal direction.

The specifications so far have not considered the attenuation with depth in the soil. Quite generally, it can be said that the high frequency components of the ground shock will be most rapidly attenuated, but since the frequency distribution is not simple and since the attenuating mechanisms are not easily predictable, no precise attenuation rules can be offered at present. N. M. Newmark of the University of Illinois has suggested an empirical form for the attenuation of pressure and vertical velocity with depth. The approximation depends on the duration of the blast impulse as approximated by the duration of a triangular pulse having the same peak overpressure and total impulse of the air blast ( $t_1$ ).

$$\frac{\sigma_d}{\Delta P_s} = \frac{v_d}{v_s} = \alpha = \frac{1}{1 + d/L}$$

where  $\sigma_d$  = earth stress at depth  $d$

$v_d$  = earth particle velocity at depth  $d$

$d$  = depth in ft

$$L = 750 t_1 \sim 300 \left( \frac{100}{\Delta P_s} \right)^{.6} W_{MT}^{1/3} \text{ ft}$$

$$\Delta P_s < 500 \text{ psi}$$

This form requires further modification for applications above 500 psi, since the high shock velocities at the higher overpressure levels tend to reduce the attenuation by the more rapid loading of larger surface areas.

$$L = 138 \left( \frac{100}{\Delta P_s} \right)^{.6} W_{MT}^{1/3} \text{ ft}$$

$$\Delta P_s > 500 \text{ psi}$$

It should be emphasized that this formula is very approximate and cannot account for wide variations in types of soil, nor does it allow for much dissipation in the soil (which at higher overpressures, particularly will be appreciable).

The presentation here is too limited for extensive discussion of design techniques in protective construction. A rather loosely connected but quite broad coverage of the various design considerations and special features is contained in the RAND Corporation report on last year's Protective Construction Symposium (R-341). I recommend it as both interesting reading and as an excellent summary and bibliographic source.

Spallation is one possible feature of strong earth shock interaction with underground cavity walls. Figure 26 schematically indicates this effect. If an impinging compressional wave is both sharp enough and strong enough to create tensions (or pressure gradients) near the cavity surface which exceed the tensile strength of the material, slabs or chips may shatter off. Spallation is less likely when the loading pulse is so broad or gradual that no large stress differences occur over distances comparable to the cavity's shortest dimension. As one goes to large yields and to large depths, the ground shock pulse should become less

P-1951  
3-31-60  
32

sharp, so that spallation may become less important than shock isolation in many applications.

### VIII. AFTER EFFECTS

Having possibly survived a near miss in a protected installation, a question of some importance to a missile system would be how soon can doors open and birds fly. Immediately following the blast wave positive phase, a negative phase sets in, in which the winds reverse and blow towards ground zero, and the overpressure becomes negative. The negative overpressure can approach as much as three psi of suction which could exert considerable lift on a sealed, pressurized installation. (A three psi partial vacuum could lift a concrete lid three feet thick!) The reversed winds may be strong enough to bring back some debris to clog openings or revetments. These winds do not stop within a few seconds, but fade right into the circulation set up by the rising fireball. Recalling the situation in the late fireball, one observes a large low density hole in the hot region. Figure 27 shows the density versus radius of this region out to a few seconds. This several thousand foot diameter low density sphere begins immediately to rise like a bubble in the atmosphere as the denser air around it forces it upwards. The rate of rise after a few seconds levels off at around 400 ft/sec. The circulation is such that the velocities in the stem that flows up through the rising cloud are about twice the cloud-rise velocities, or as much as 800 ft/sec. The consequences of such wind velocities can be better appreciated when one considers that the drag created by this flow could hold aloft as much as a seven ton boulder, or could loft lesser rocks and debris to very high altitudes. The cloud continues to rise for four to six minutes, which takes it to altitudes upwards of sixty thousand feet,

dependent on meteorology. Even after the cloud has stabilized, the stem continues to rise as the circulation persists. During the time of the initial cloud rise much of the cratered debris is aloft on various trajectories, and much of this material will be excavated at pressures below that needed to pulverize or vaporize the rock or soil, some of it will be lofted in essentially its original sizes and shapes. If the soil is rocky, then some rocky throwout may be carried up. Consequently, since the stem of the cloud extends out far beyond the 100 psi distance from a one megaton burst, there is some chance that rocks may rain down over a wide area for many minutes after a burst.

Again, if the wind circulation closely corresponds to the visible cloud and stem movements, one may expect wind velocities of the same order of magnitude ( $\sim 100$  ft/sec) at the base of the stem, i.e. in the dust-laden air above a 100 psi shelter.

Visibility will be restricted and unpredictable over an area corresponding to at least the 10 psi distance from such bursts, so that visual assessment of the post-burst external environment will not always be possible. Direct human exposure would be undesirable, possibly even fatal, in the local fallout, which outside the immediate crater area (but within 10 or so miles) can still run to thousands of roentgens per hour in the first few hours to a few hundred at the end of a day. Total doses (integrated over time) after 18 hours may be in excess of 3000 r over a thousand square miles. Clearly, surviving nearby surface installations or support structures will not be habitable for many hours after a megaton weapon surface burst even in extreme emergencies.

The persistence of unfavorable after-effects, which may be so dangerous as to prohibit normal launch procedures, suggests that serious thought be given to designing missile systems with sufficient protection to ride out in safety an anticipated attack, and thus avoid the many difficulties in carrying out a prompt response. At least one is required to carefully assess the penalties which must accompany a specified fast response where the fast response is to apply also after a bomb has struck.

## SHOCK INFLUENCE ON PROMPT GAMMA-RAYS

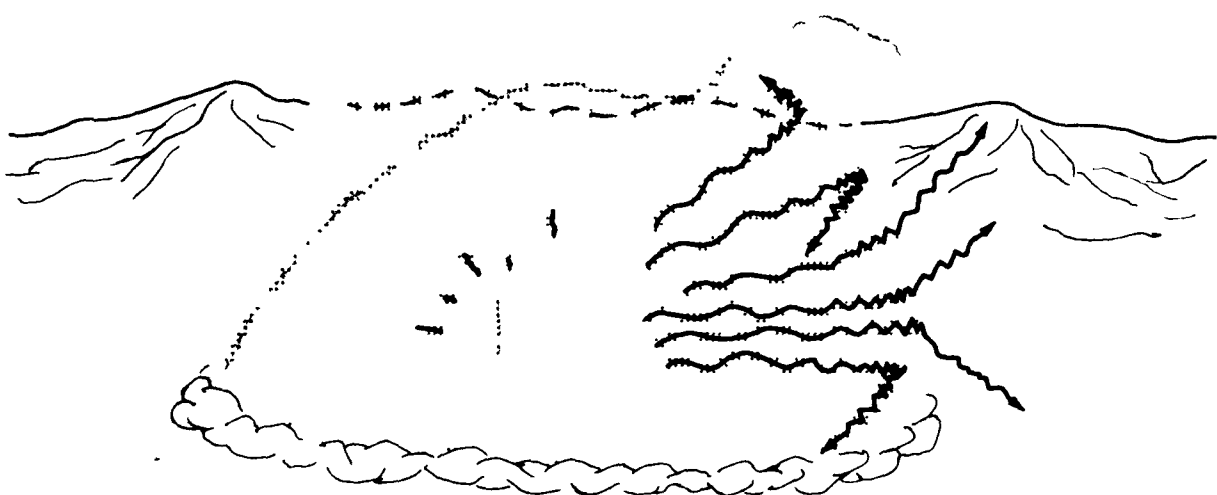


Fig. 1. Shock Influence on Prompt Gamma Rays

The fission fragment gamma-rays travel with little attenuation through the partial vacuum of the fireball interior but absorb and scatter strongly in the dense air just behind the shock front, and attenuate normally in the undisturbed air ahead of the shock.

## HALF-THICKNESSES FOR GAMMA RAY ATTENUATION

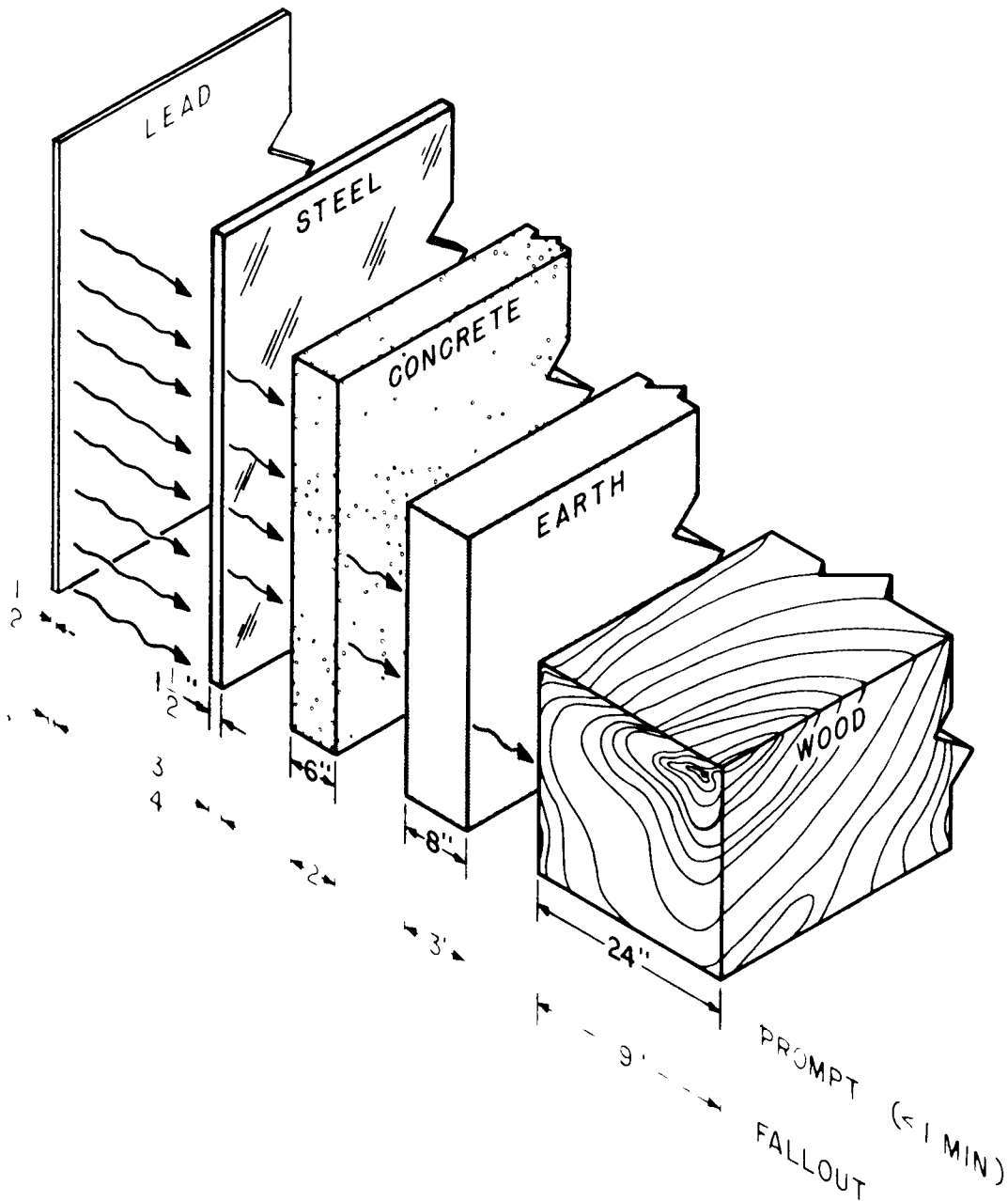


Fig. 2

FIREBALL TEMPERATURE VS RADIUS AT EARLY TIMES  
ONE MEGATON—SURFACE BURST

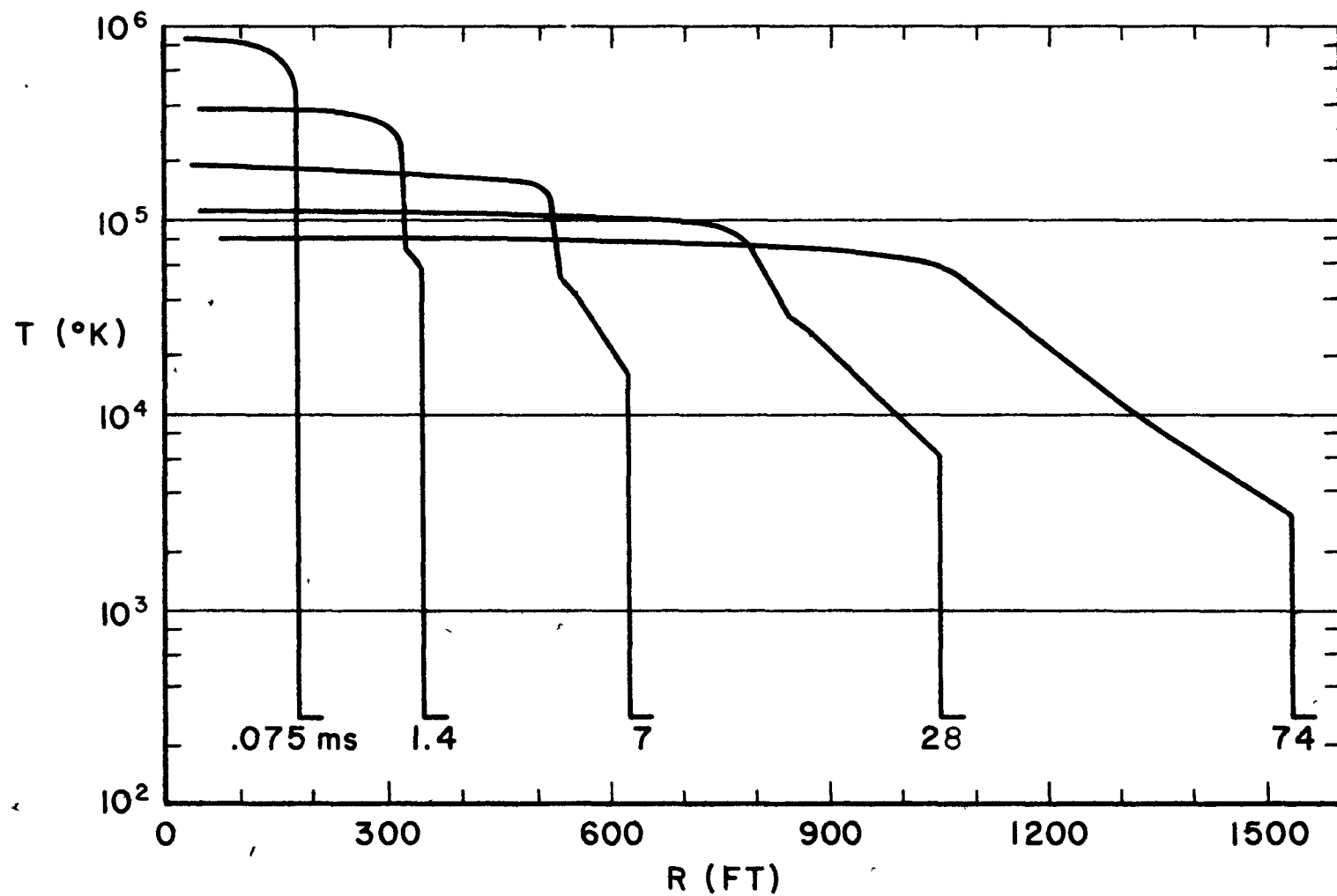


Fig. 3

85-11-21  
PAGE 1  
100%

FIREBALL DENSITY VS RADIUS AT EARLY TIMES  
ONE MEGATON—SURFACE BURST

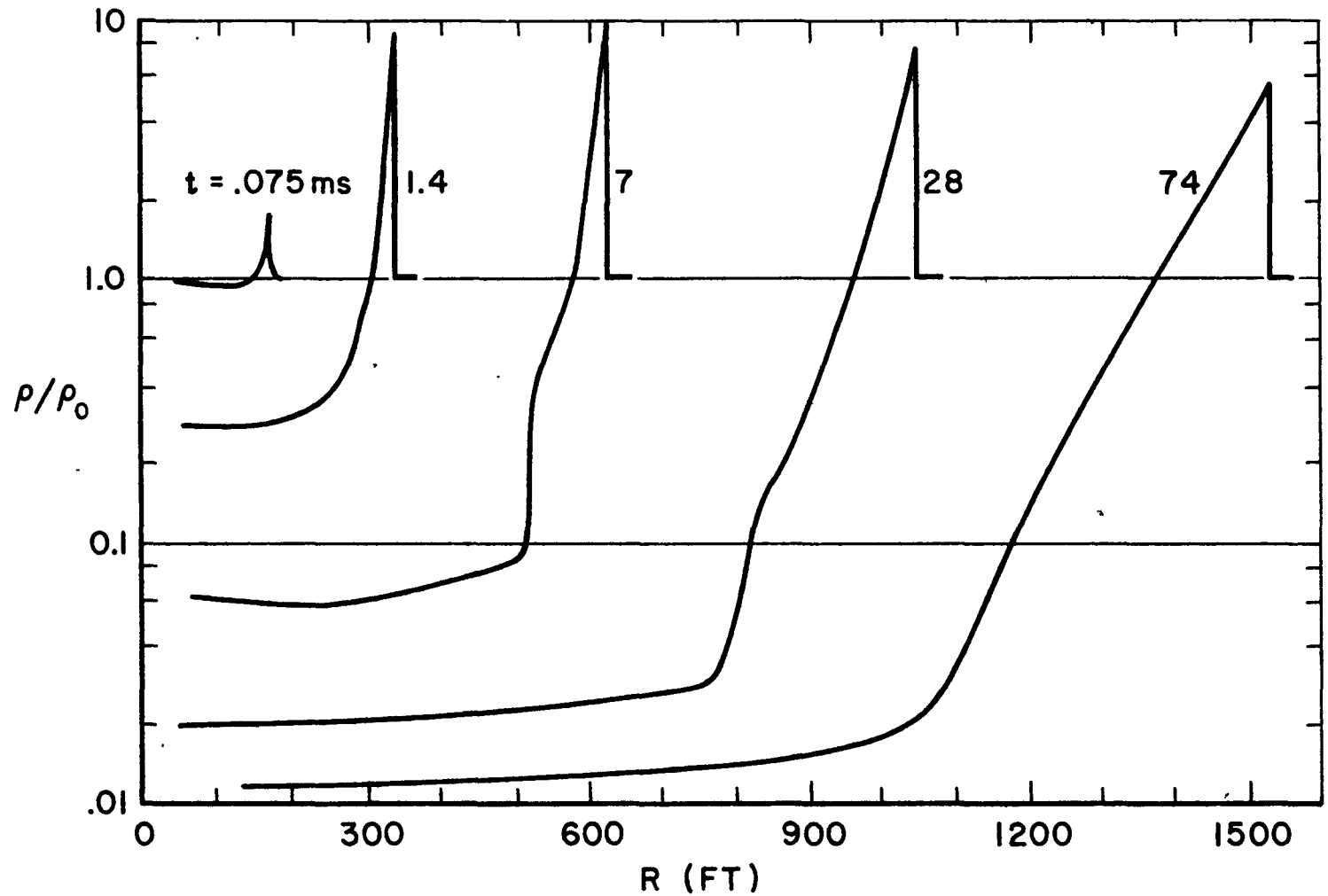


Fig. 4

66-TR-4  
1661-4

FIREBALL OVERPRESSURE VS RANGE AT EARLY TIMES  
ONE MEGATON—SURFACE BURST

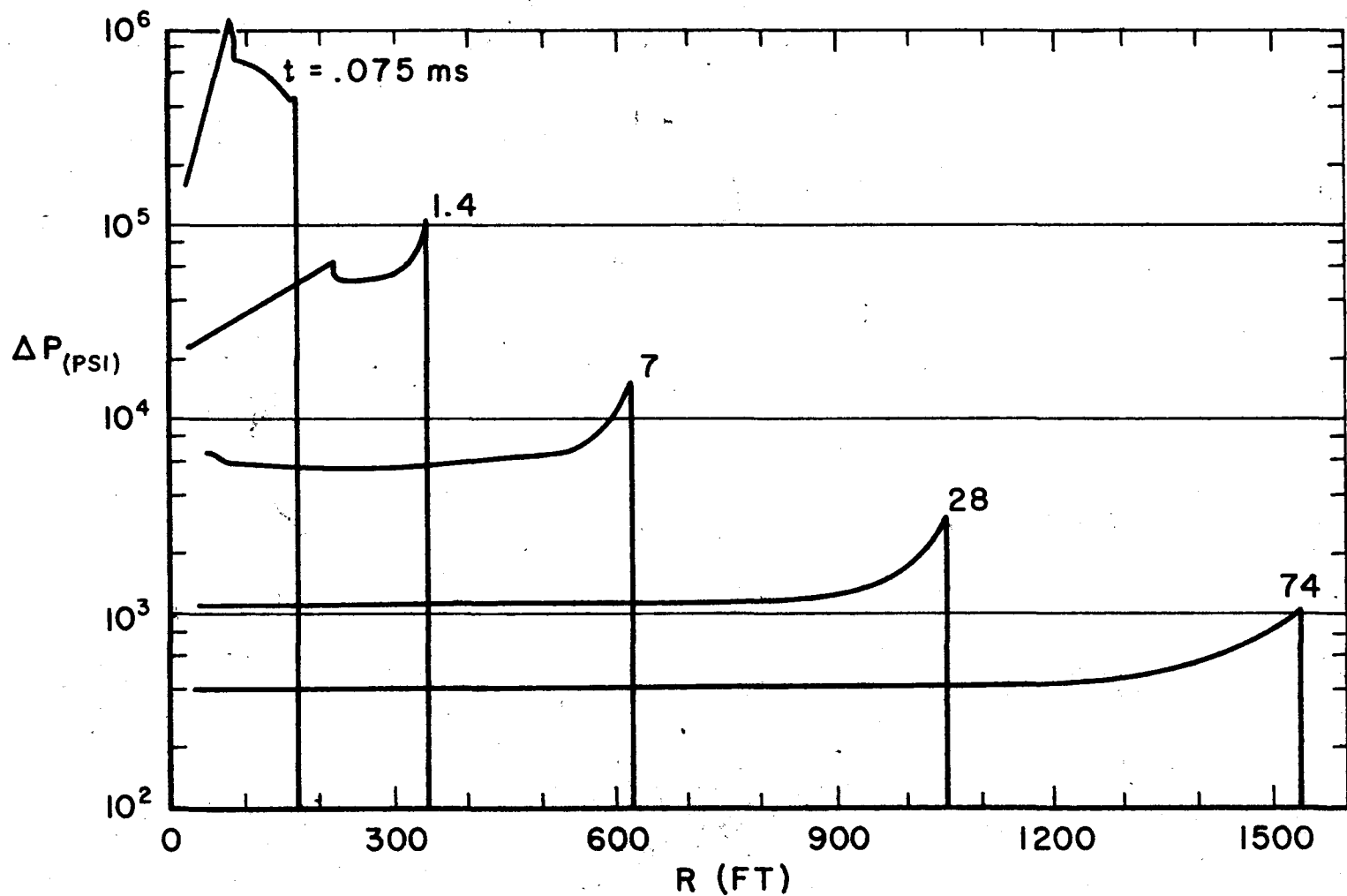


Fig. 5

LATE FIREBALL TEMPERATURE VS RADIUS  
ONE MEGATON— SURFACE BURST

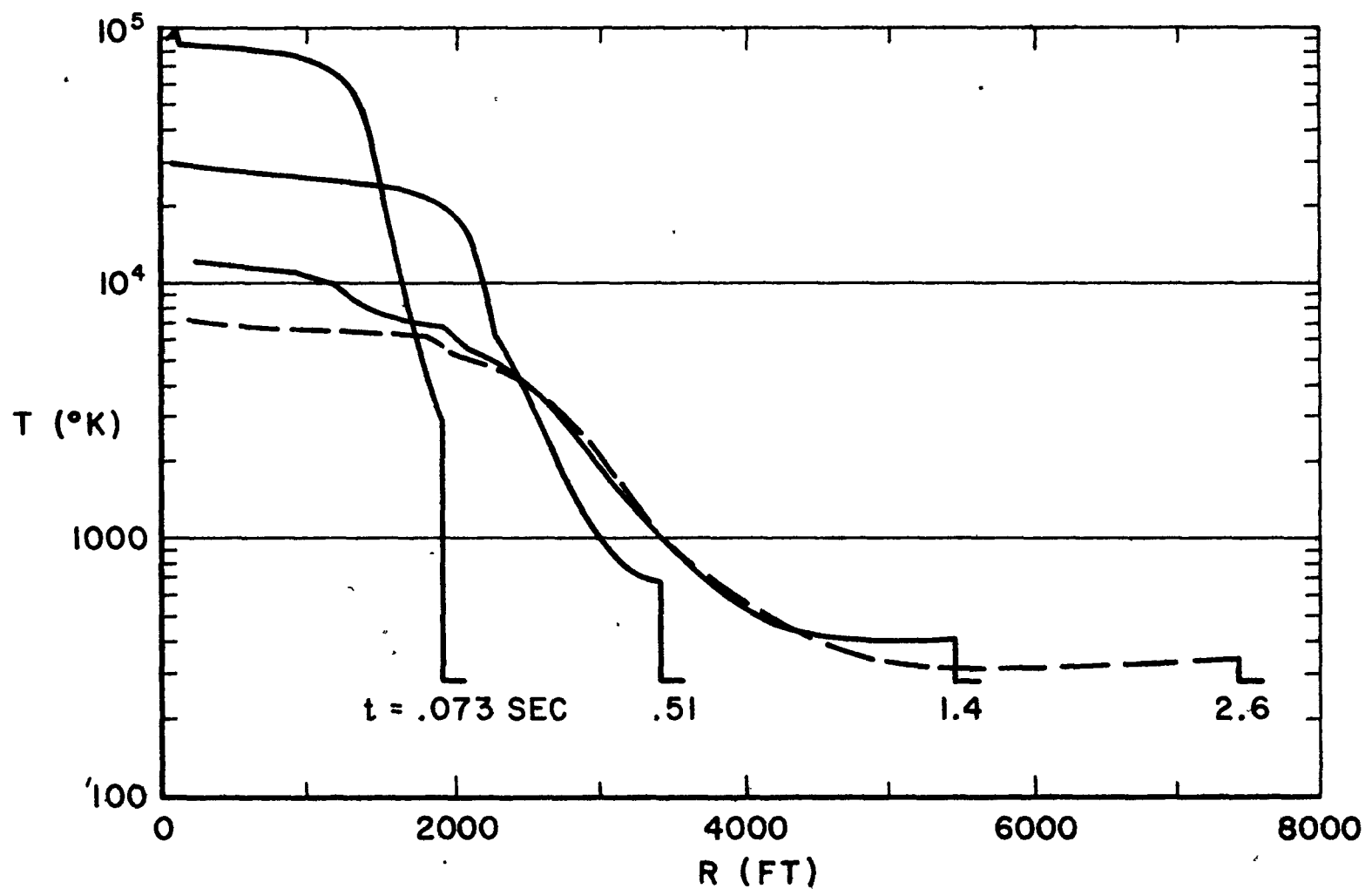


Fig. 6

# TEMPERATURE VS TIME AT HIGH PEAK OVERPRESSURES

ONE MEGATON — SURFACE BURST

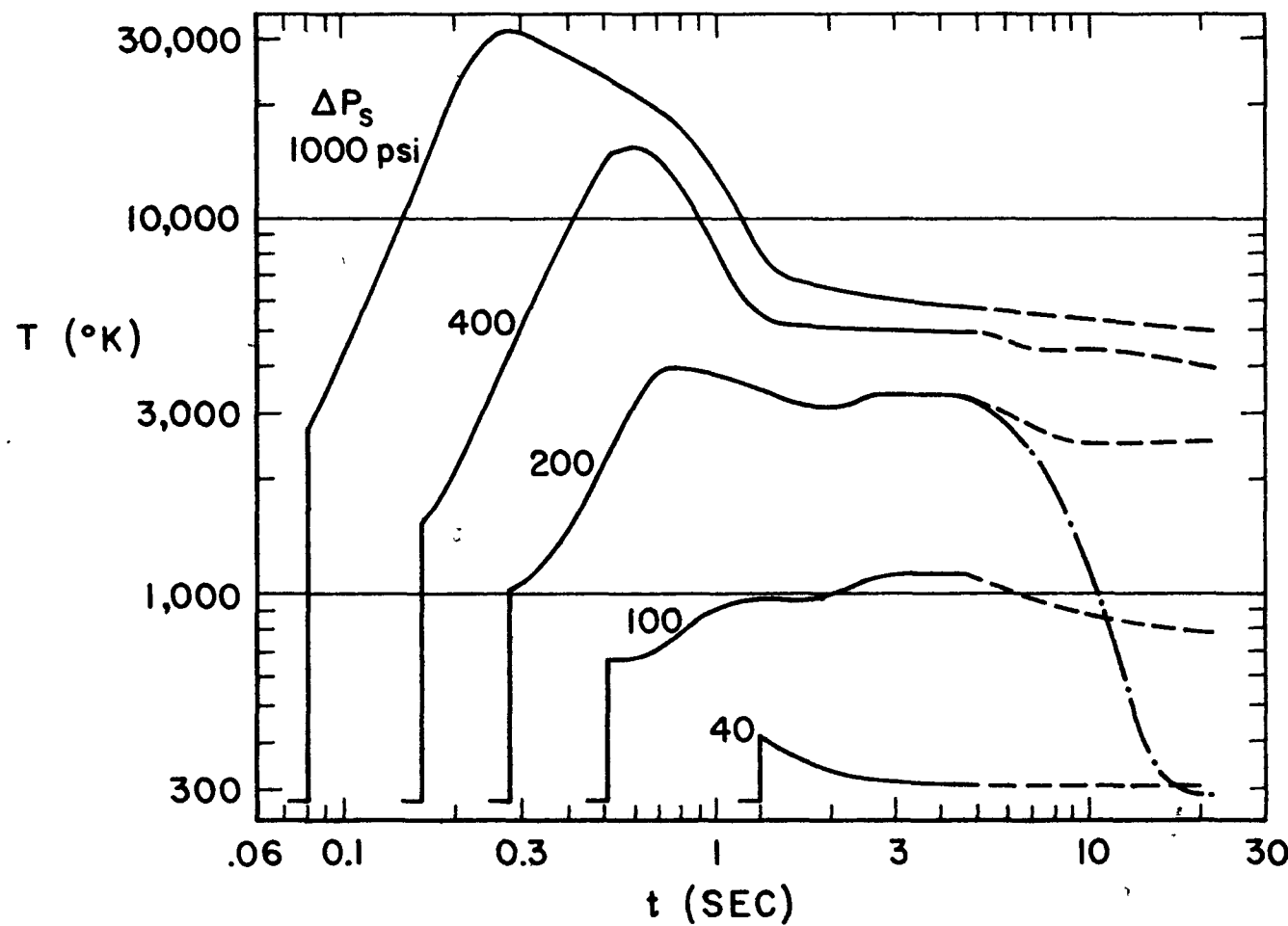


Fig. 7

4-1951  
3-31-68

OVERPRESSURE VS RADIUS  
ONE MEGATON— SURFACE BURST

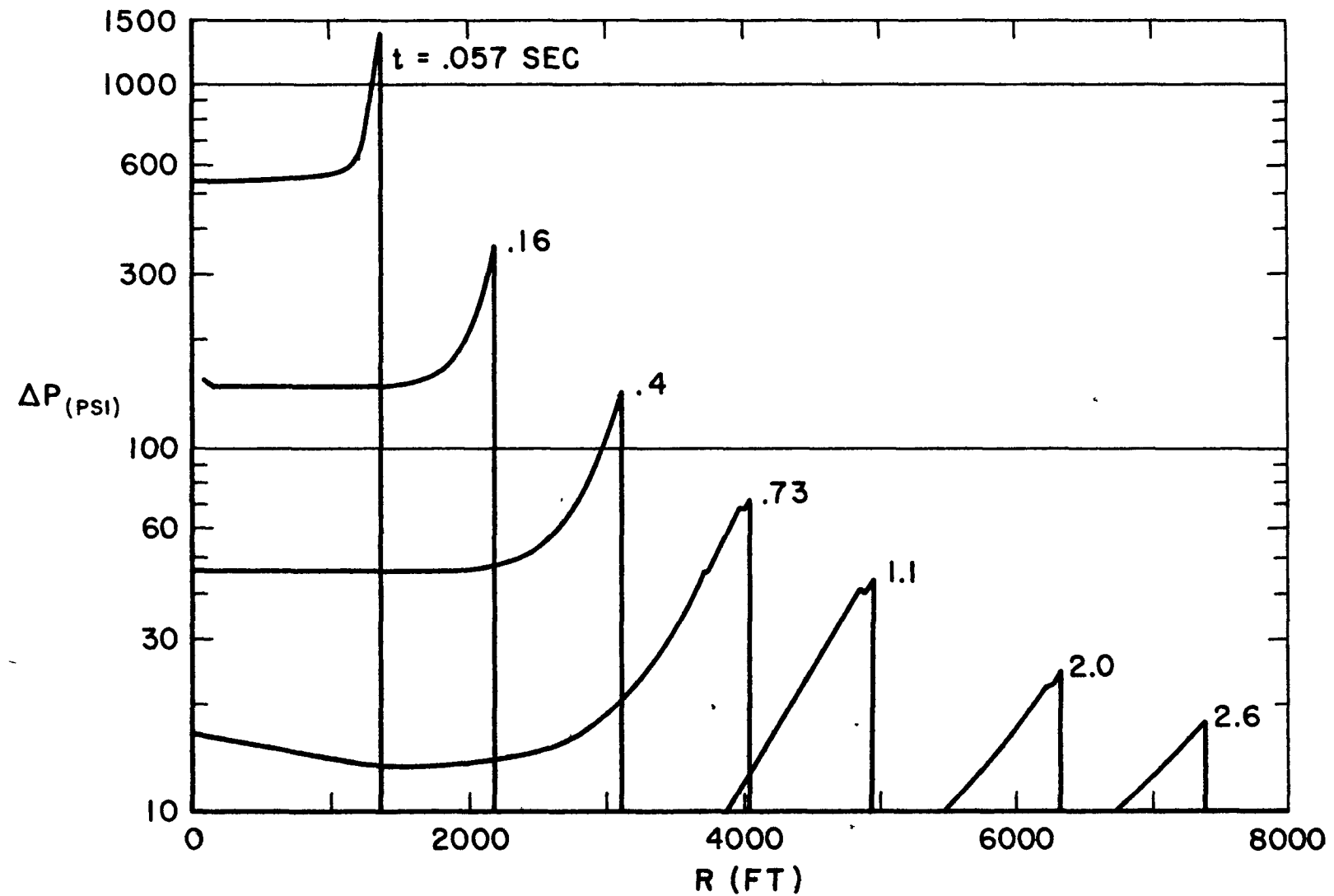


Fig. 8

59-15768

P-1951  
3-31-60  
44

## OVERPRESSURE VS TIME ONE MEGATON—SURFACE BURST

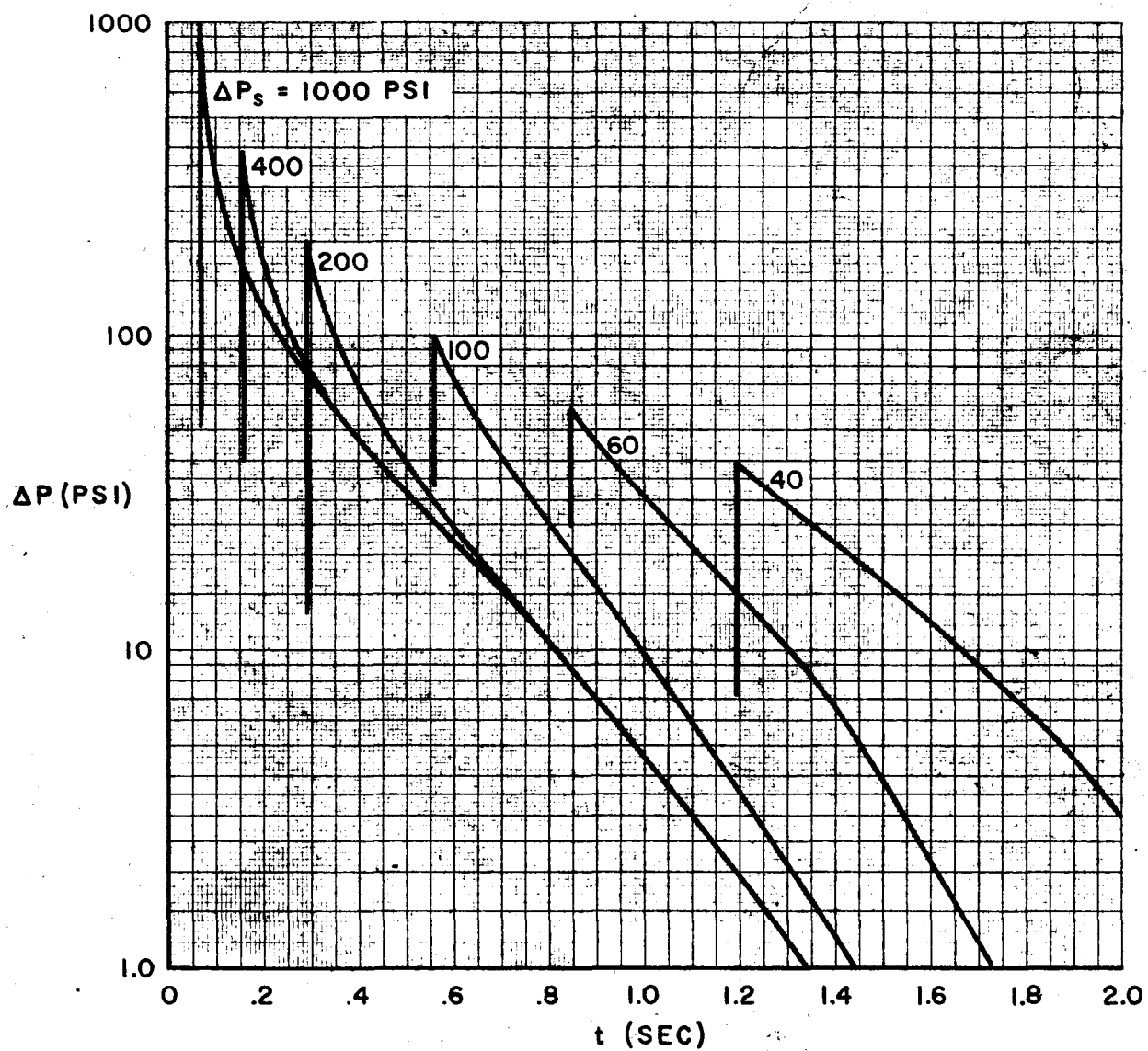


Fig. 9

P-1951  
3-31-60  
45

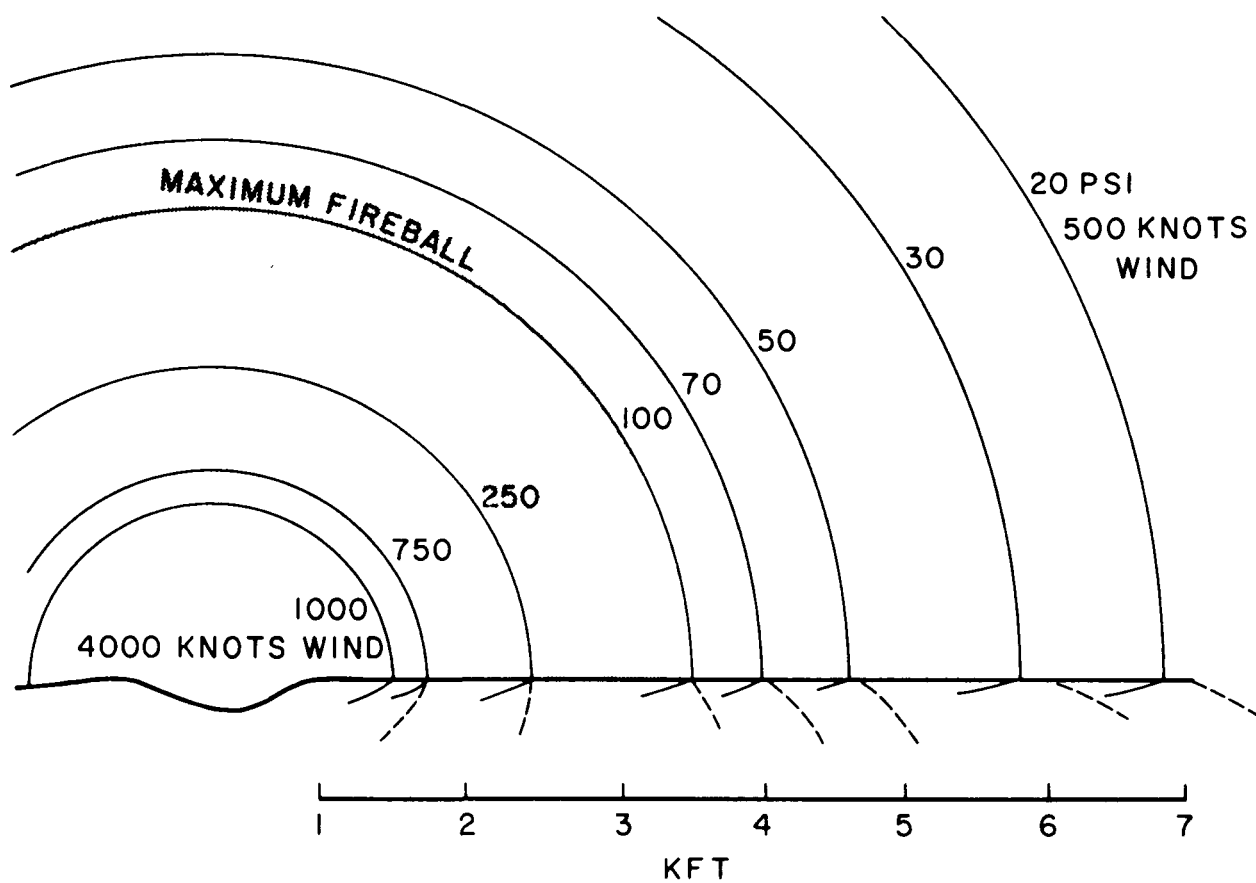


Fig. 10

P-1951  
3-31-60  
46

## SHOCK PARAMETERS VS SHOCK OVERPRESSURE

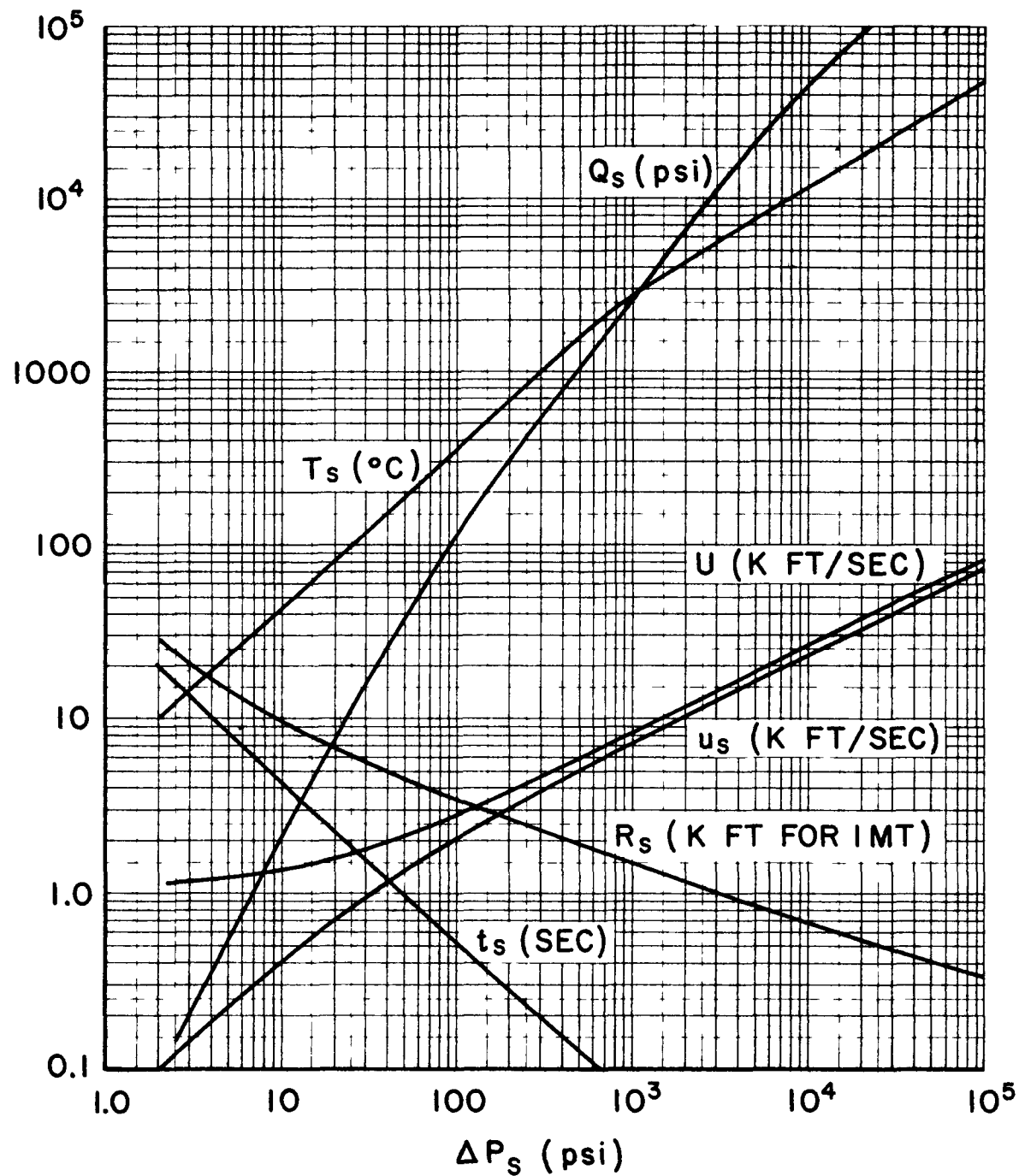


Fig. 11

P-1951  
3-31-60  
47

## IMPULSES AND DURATIONS IN POSITIVE PHASE OF OVERPRESSURE

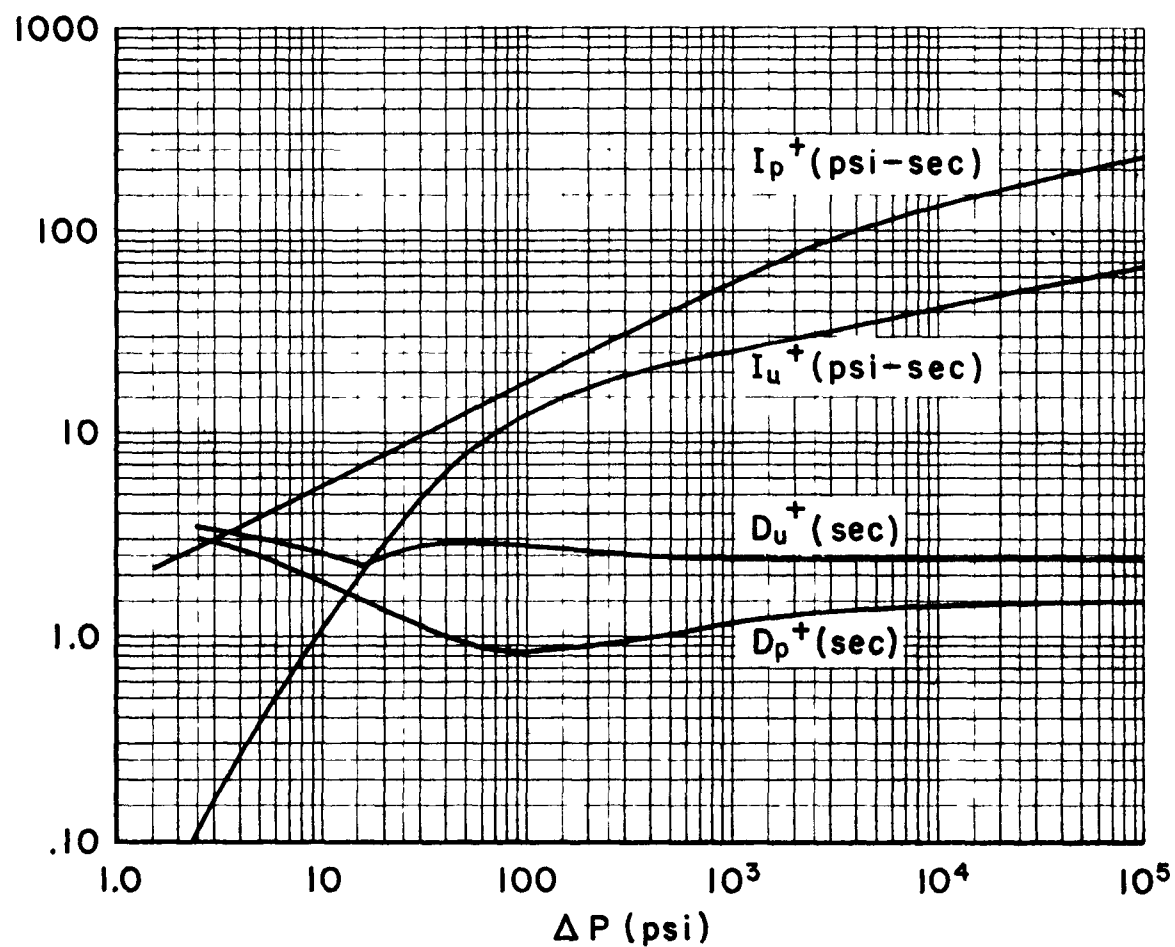


Fig. 12

P-1951  
3-31-60  
48

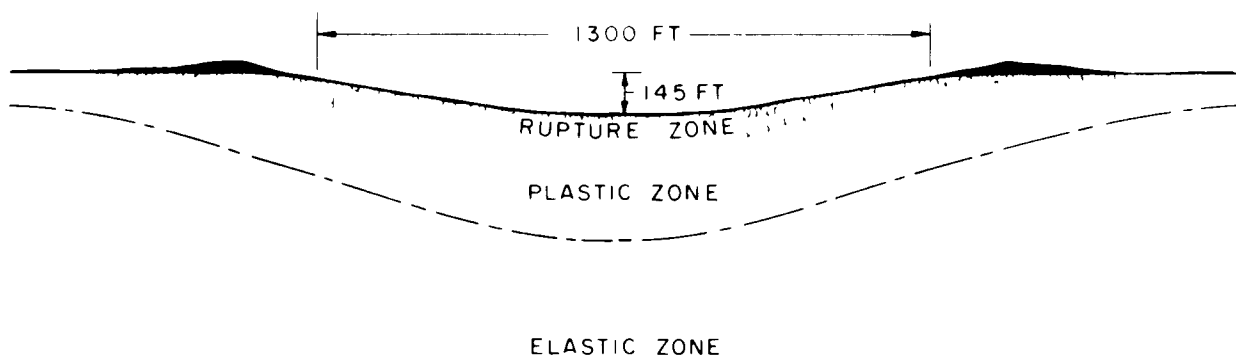


Fig. 13

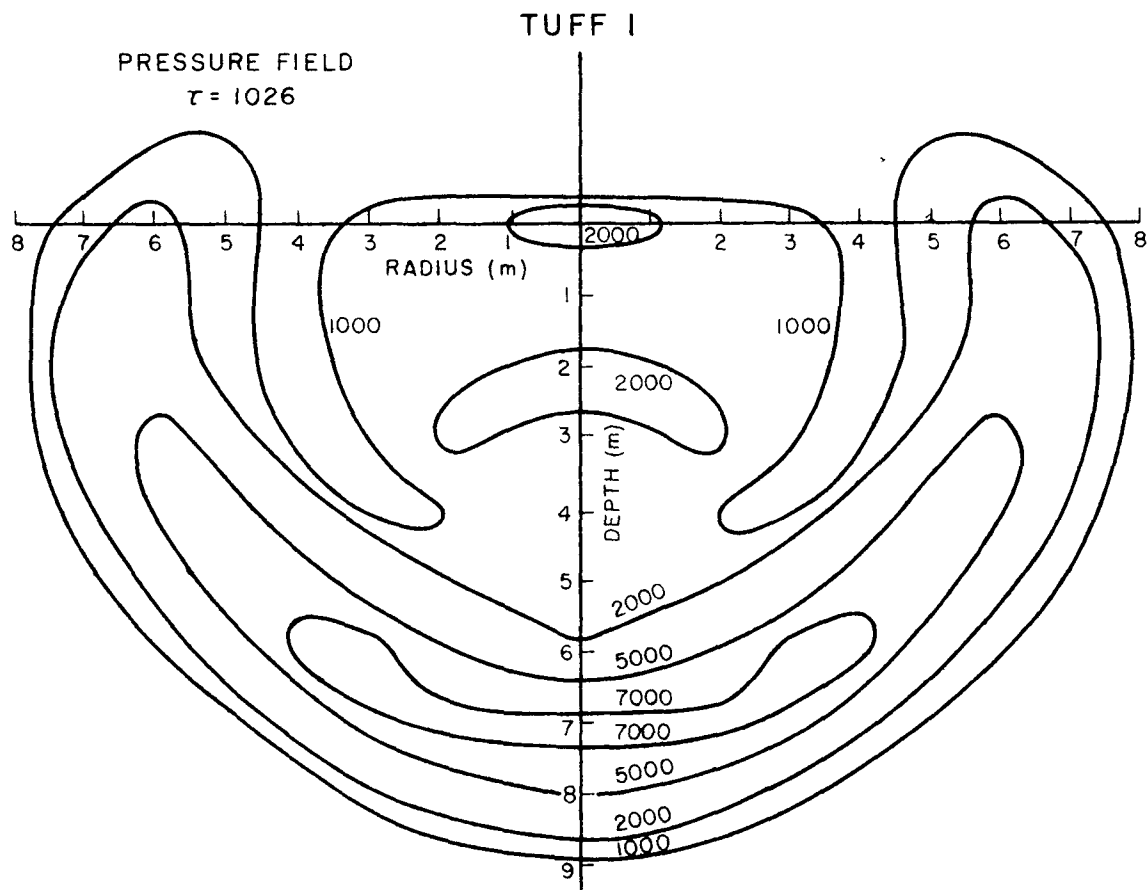


Fig. 14

64  
 09-15-73  
 T567-4

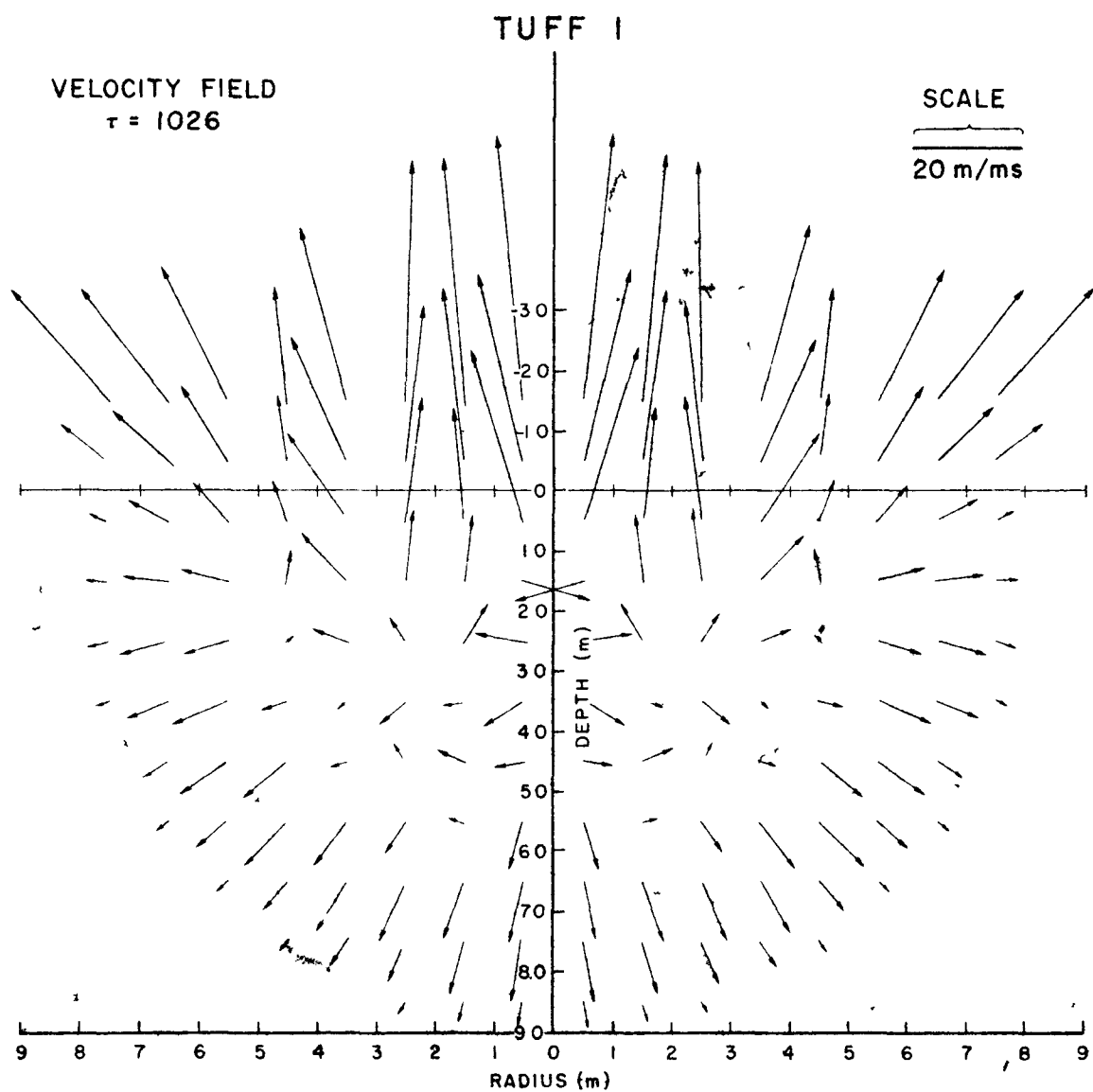


Fig. 25

P-1951  
3-31-60  
51

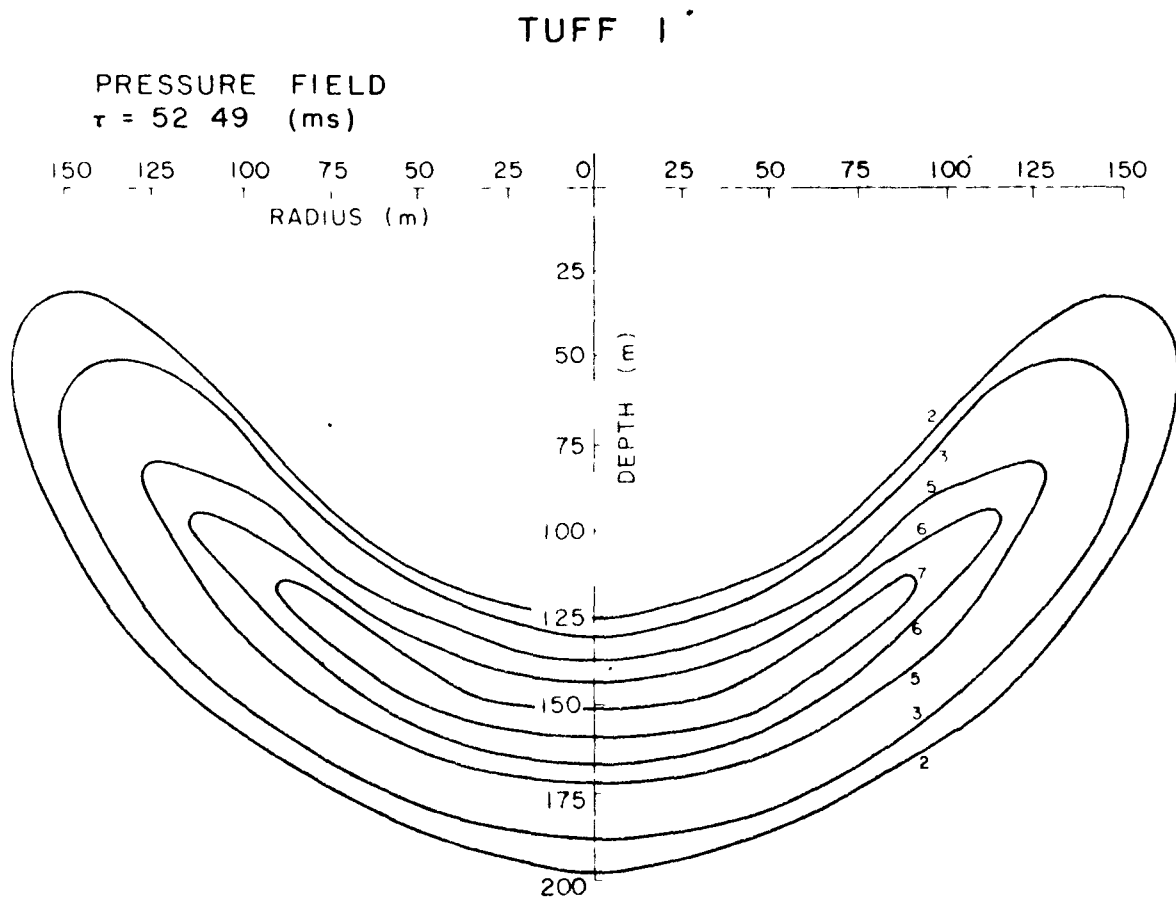


Fig. 16

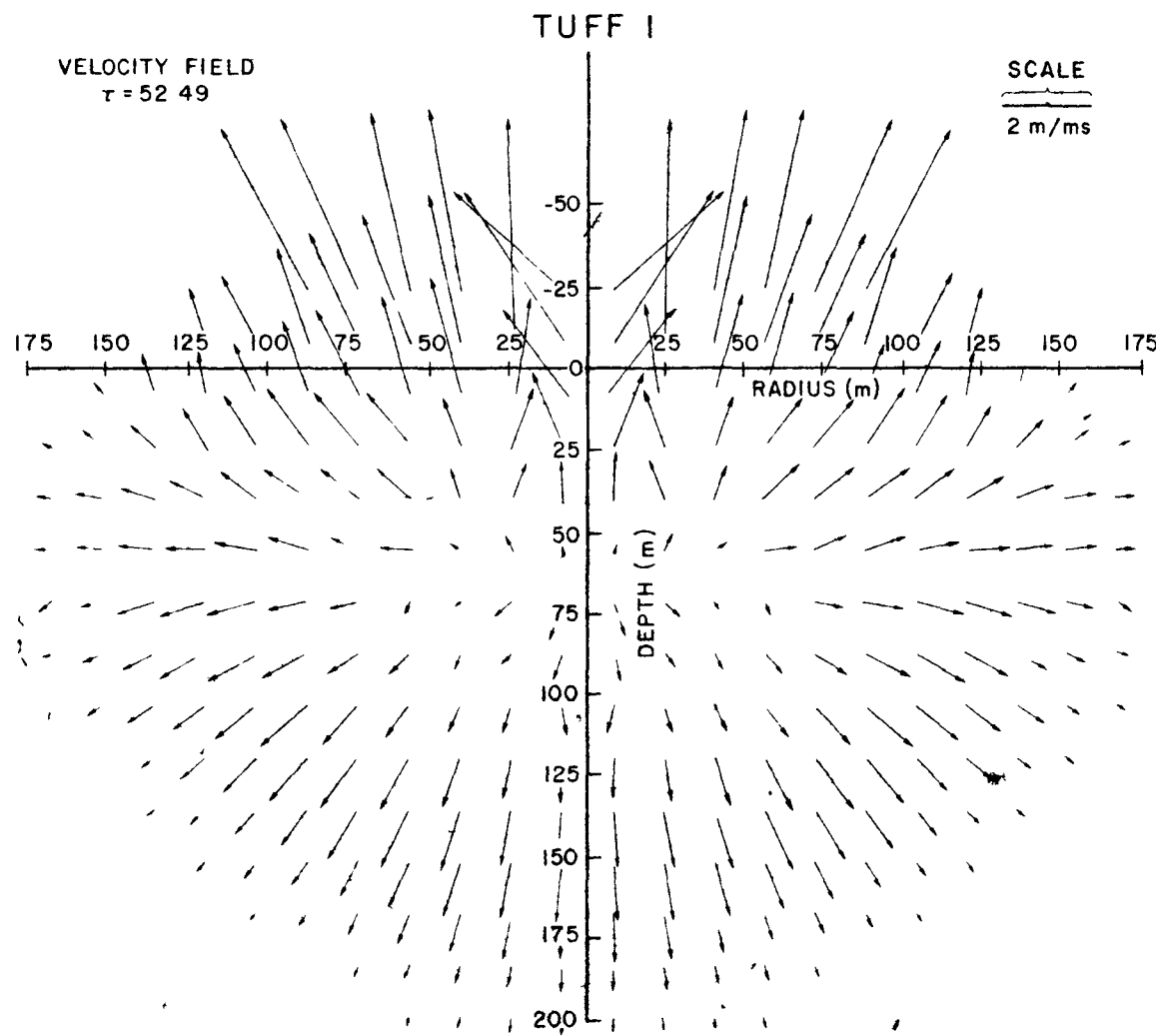


Fig. 17

TUFF 1

PRESSURE FIELD  
 $\tau = 105$  ms

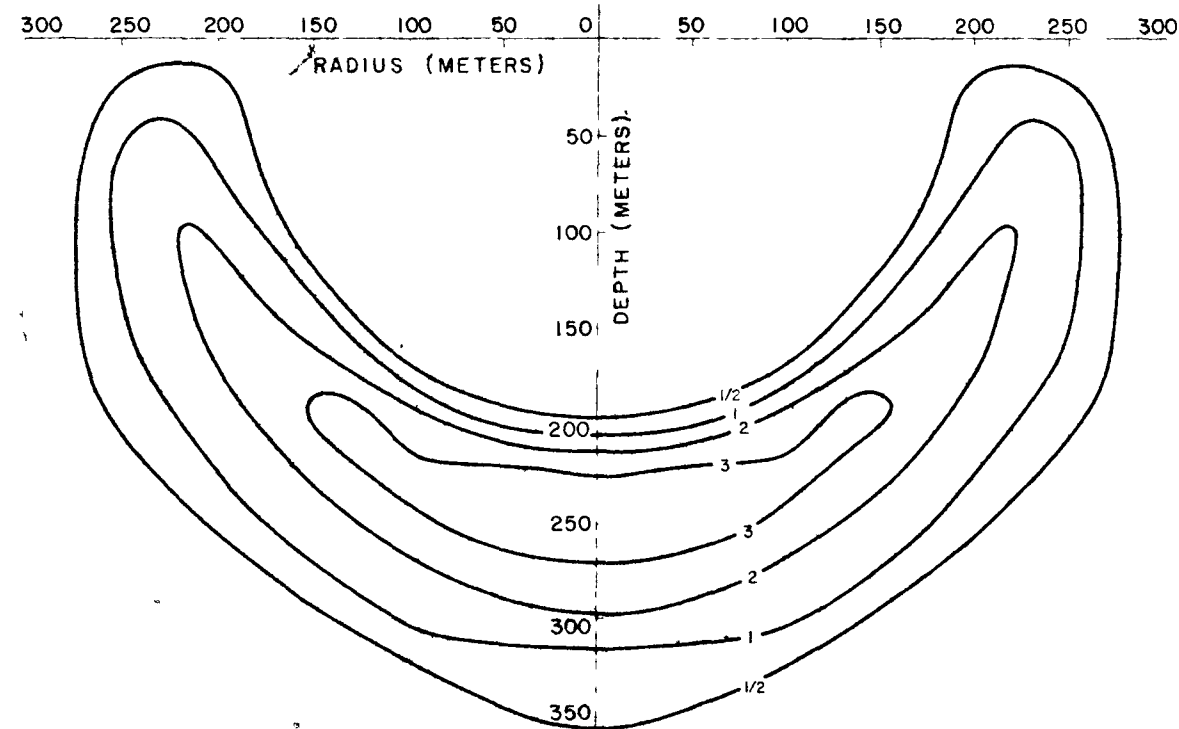


Fig. 18

55  
09-11-74  
TEST-2

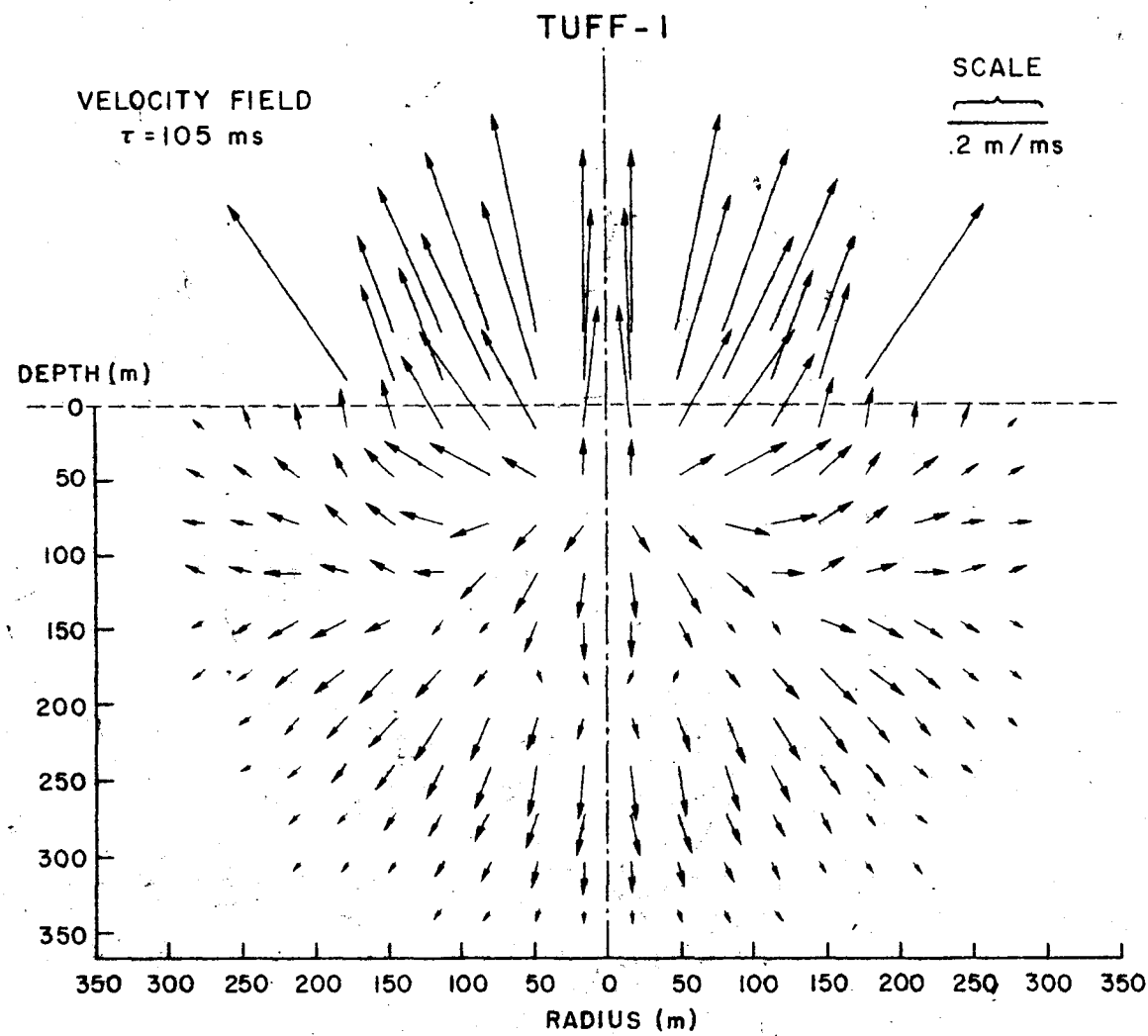


Fig. 19

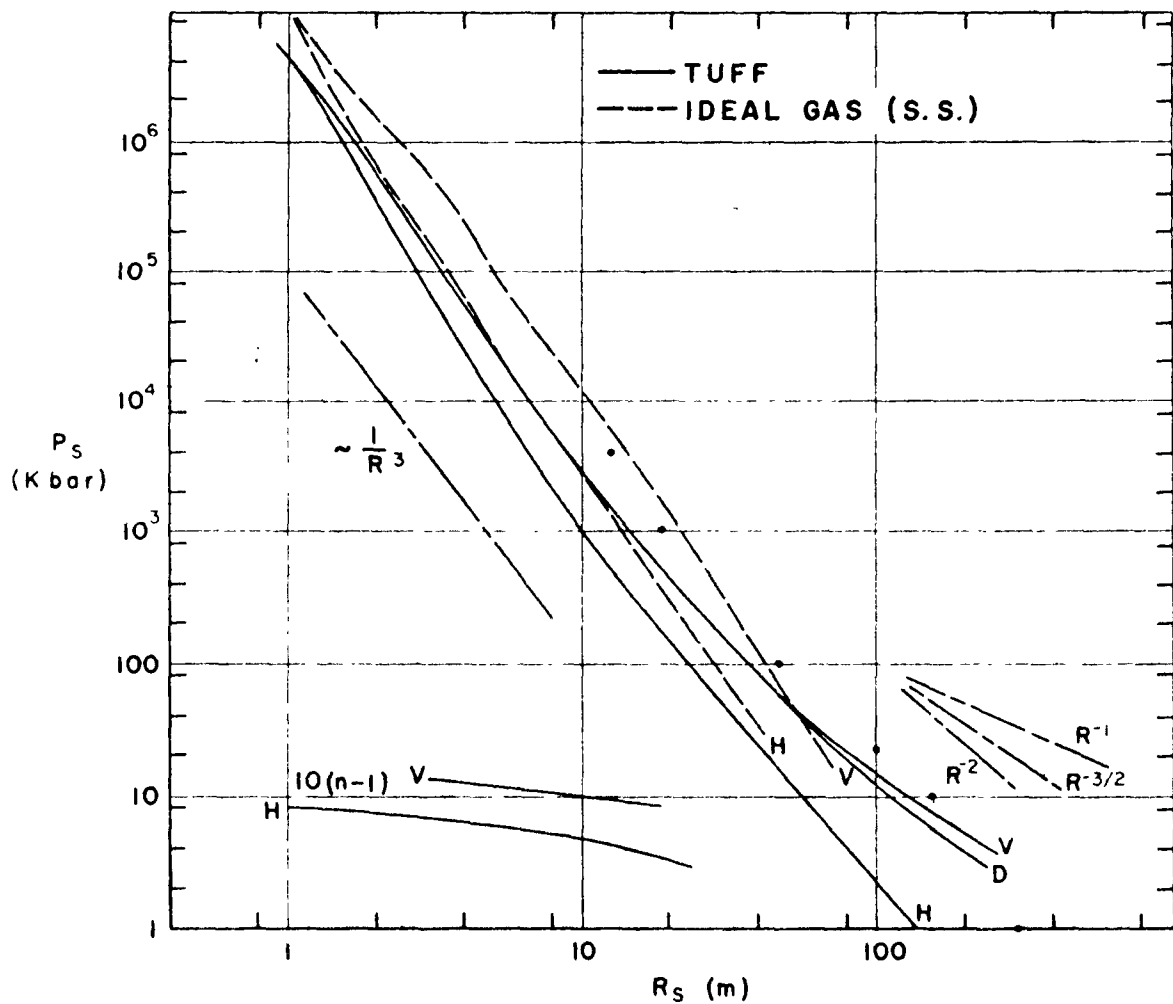


Fig. 20

P-1951  
3-31-60  
56

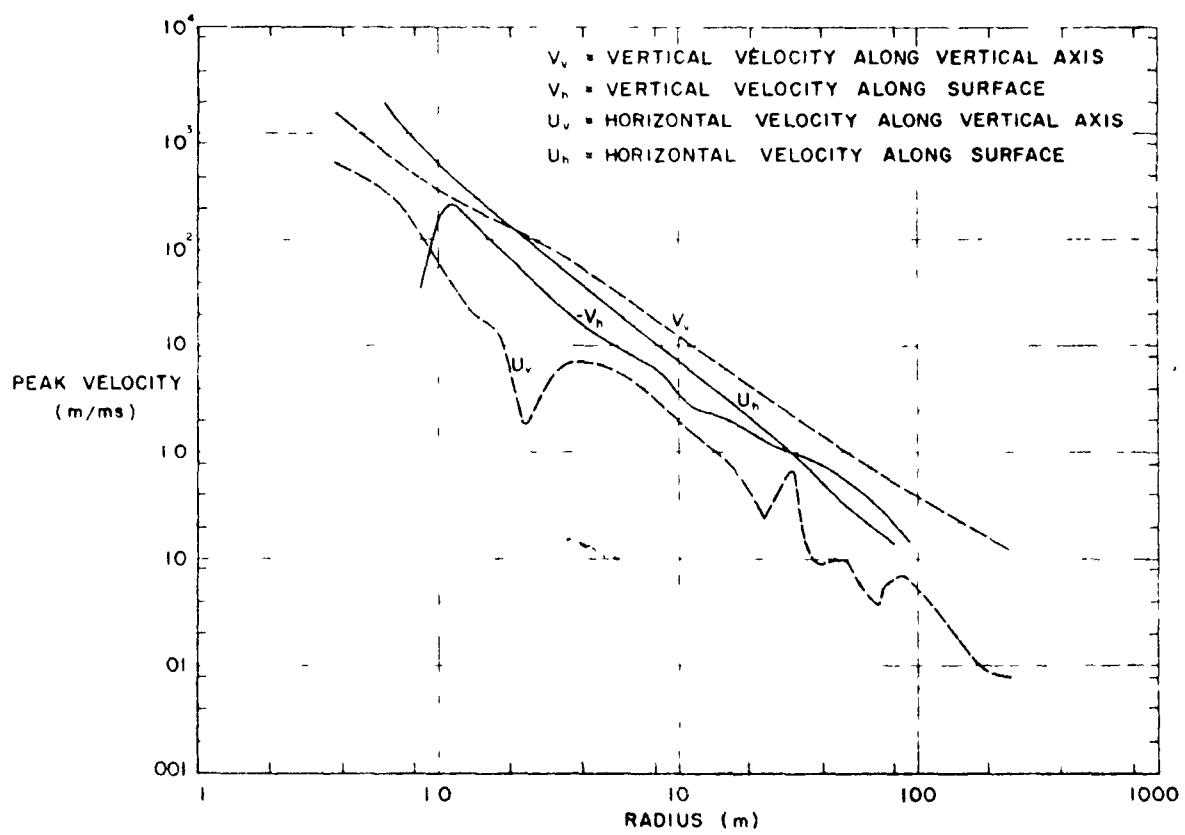


Fig. 21

P-1951  
3-31-60  
57

ONE MEGATON — 1000 PSI  
.077 SECONDS, 1500 FT RADIUS

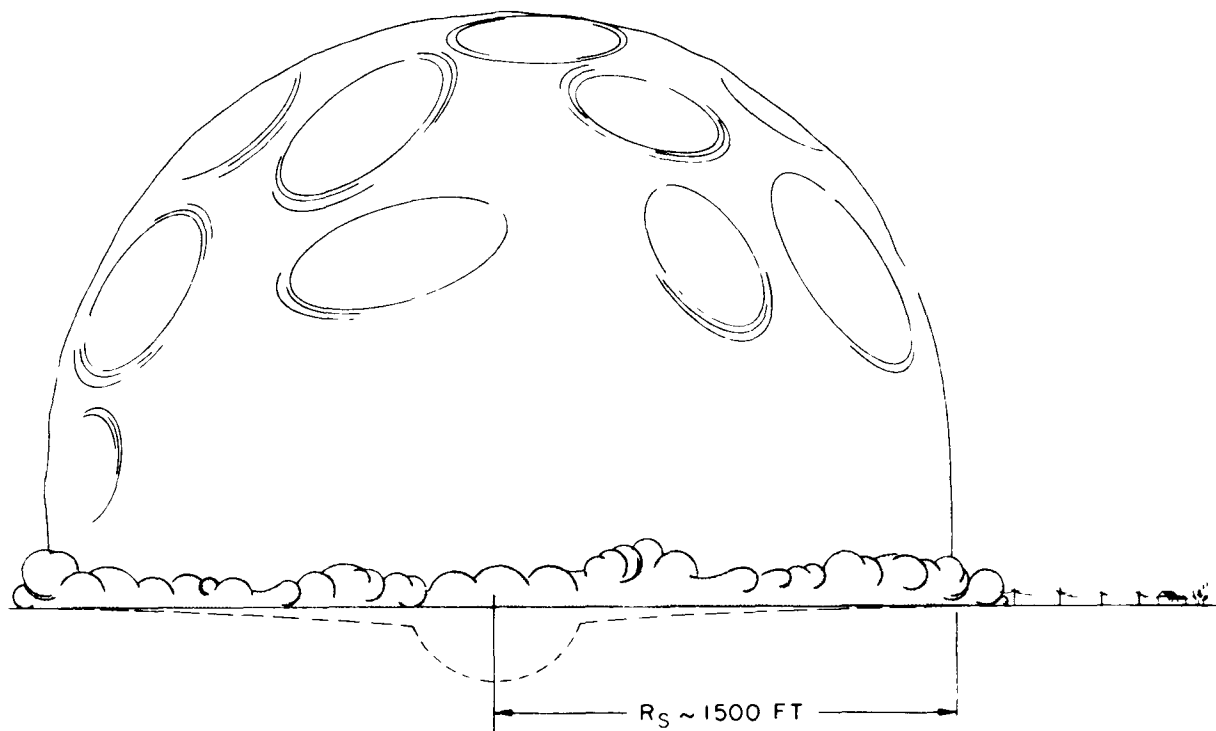


Fig. 22

### VERTICAL ACCELERATIONS AT SHALLOW DEPTHS

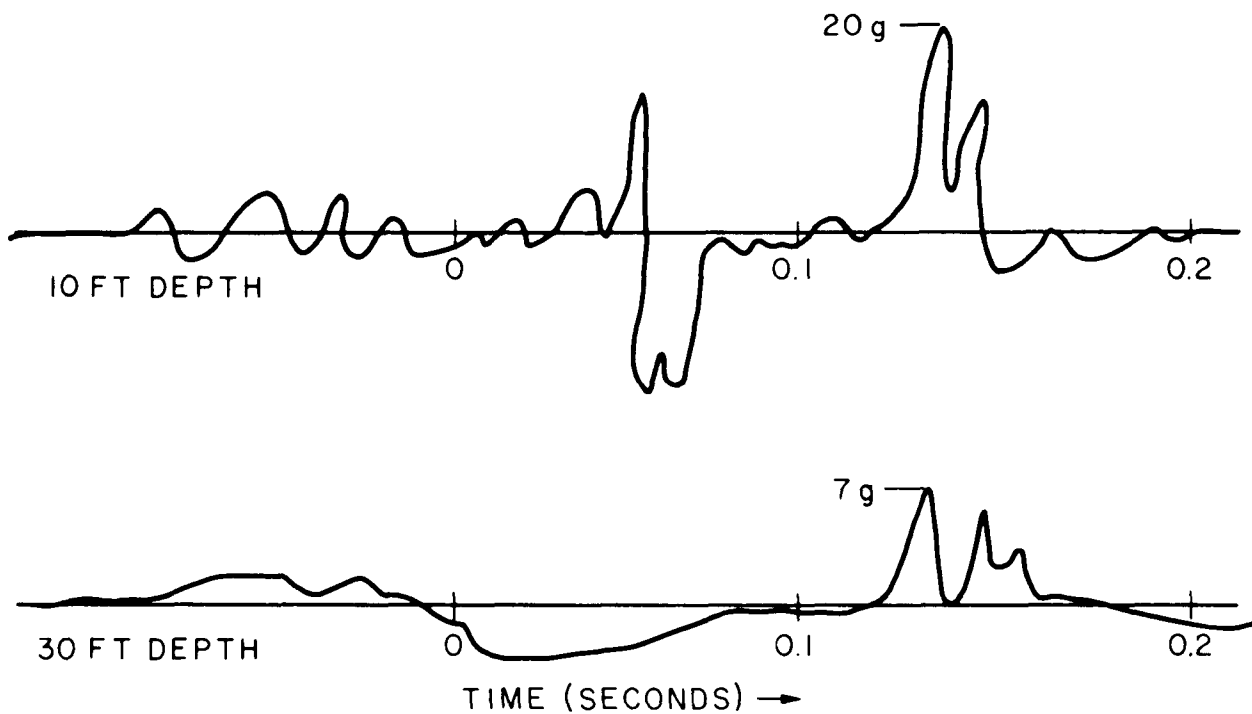


Fig. 23

## VERTICAL SHOCK SPECTRA

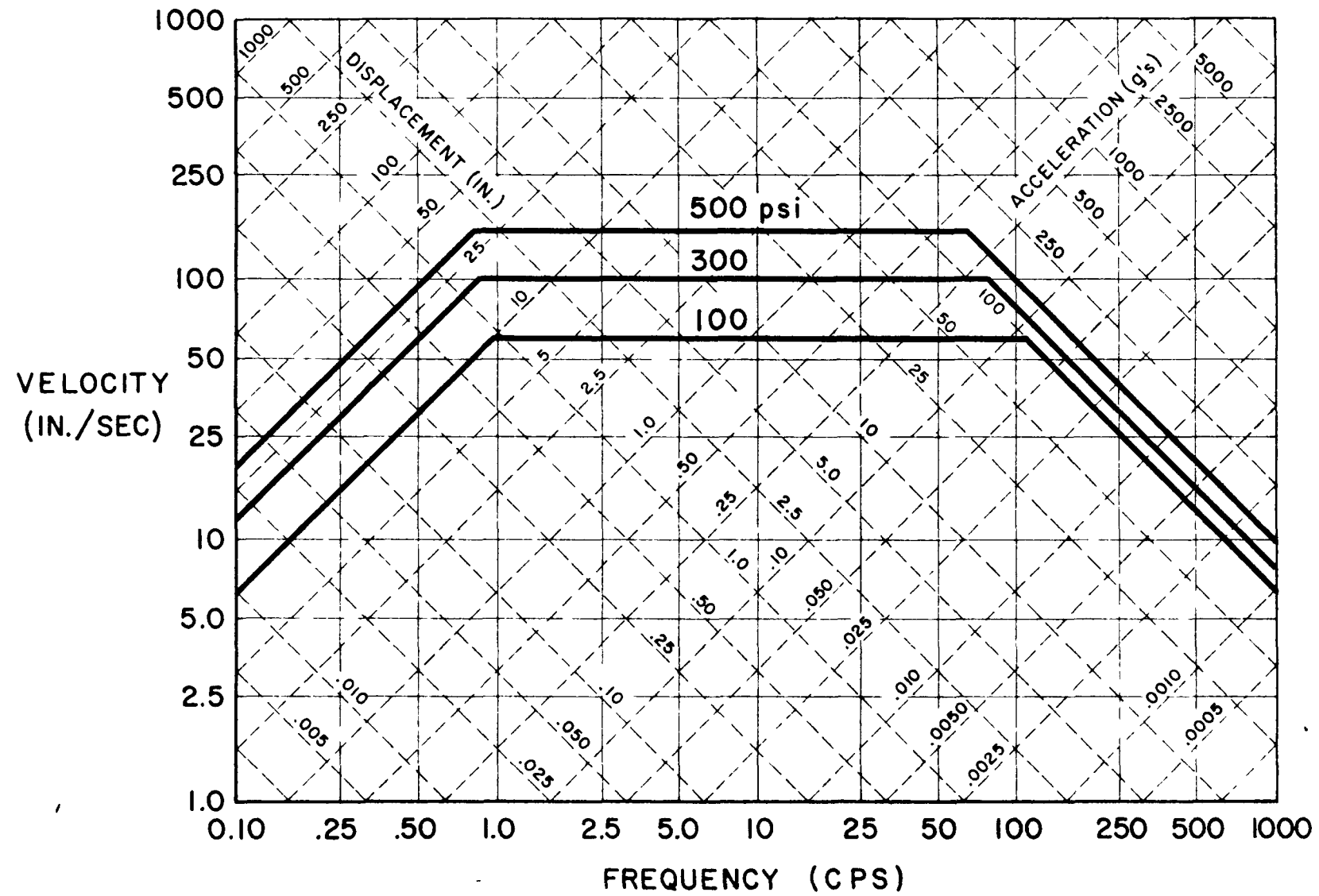


Fig. 24

65  
OCT 1962  
TEST

## HORIZONTAL SHOCK SPECTRA

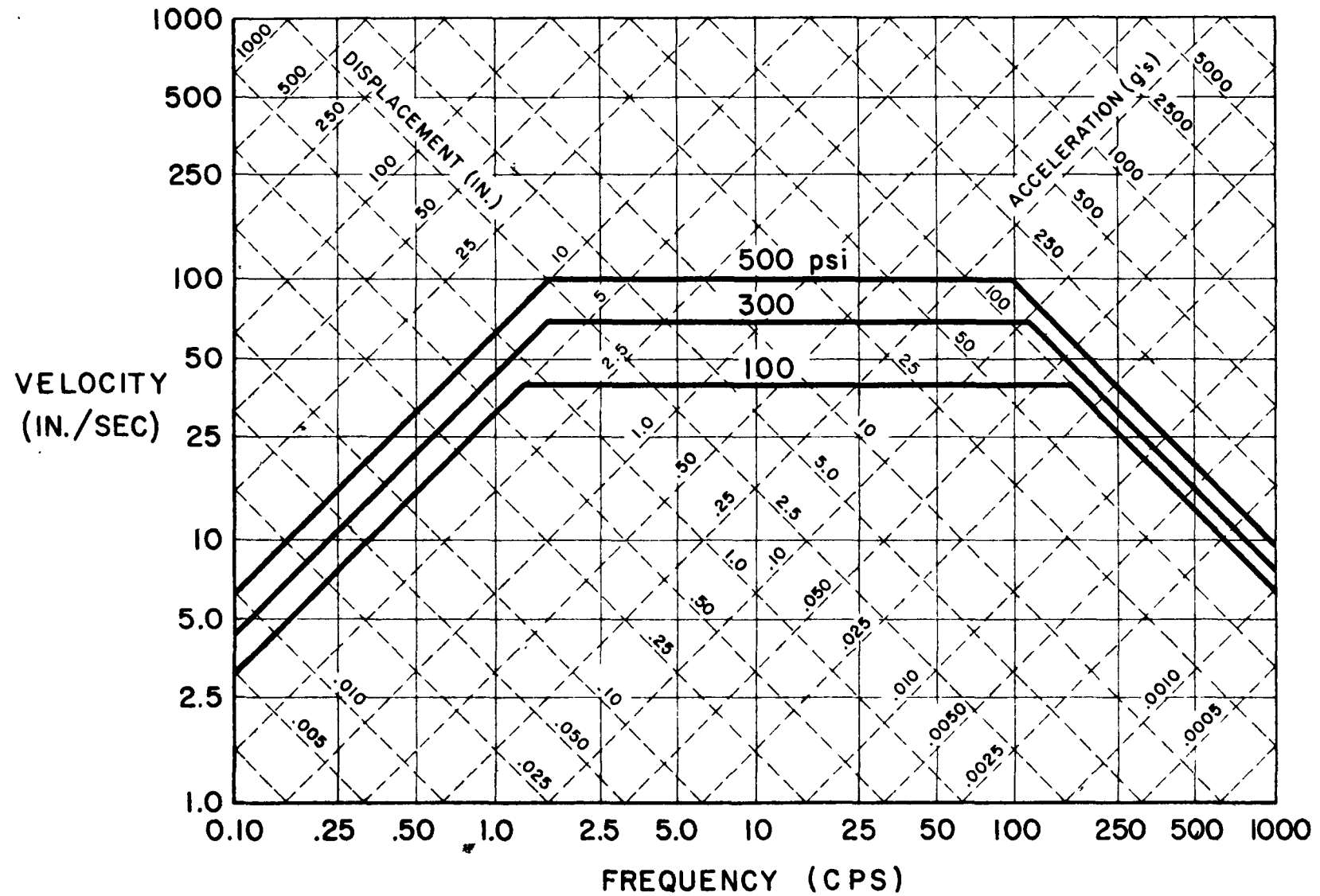


Fig. 25

66-5575  
Ref. 1

P-1951  
3-31-60  
61

## SPALLATION

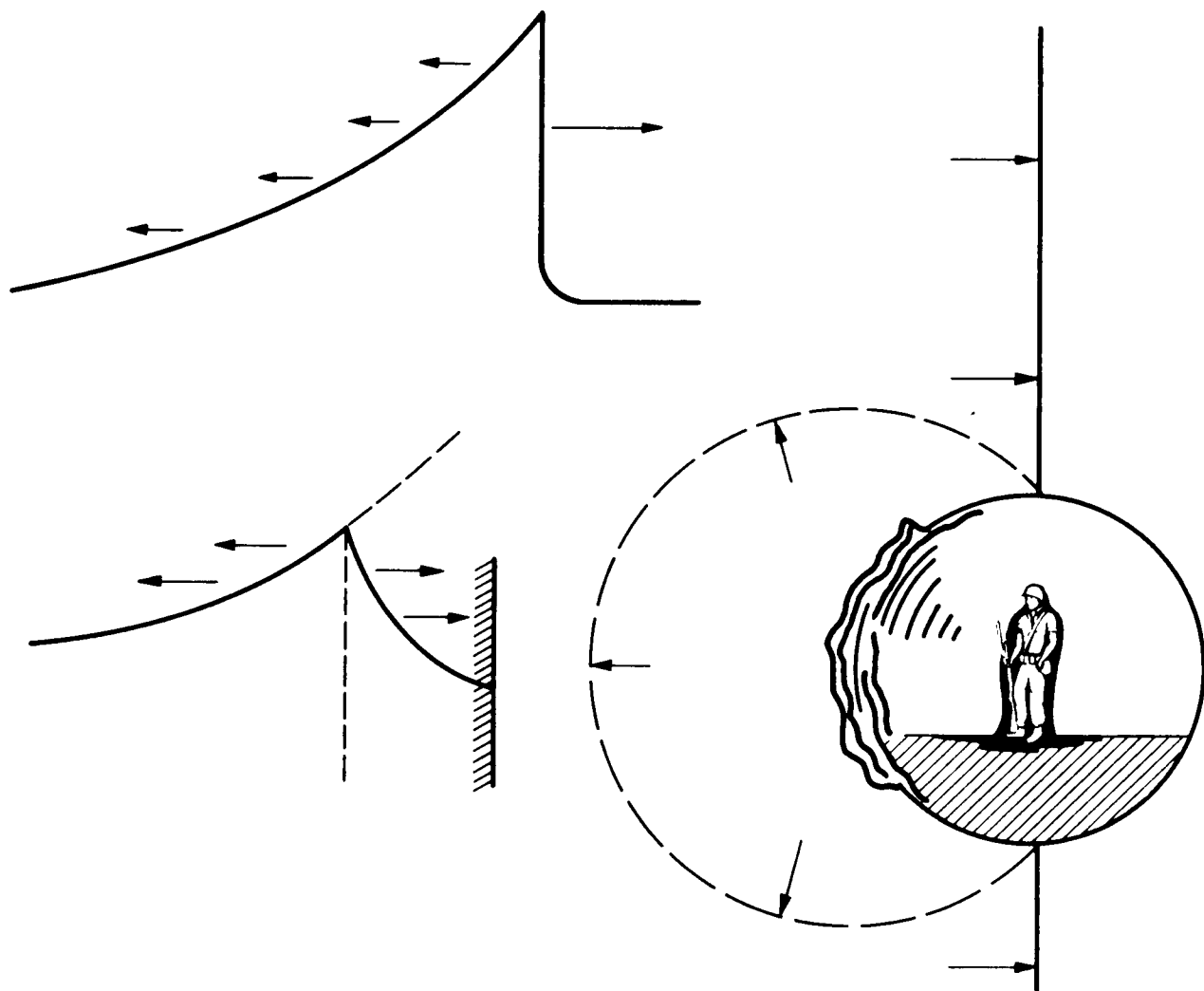


Fig. 26

LATE FIREBALL DENSITIES  
ONE MEGATON—SURFACE BURST

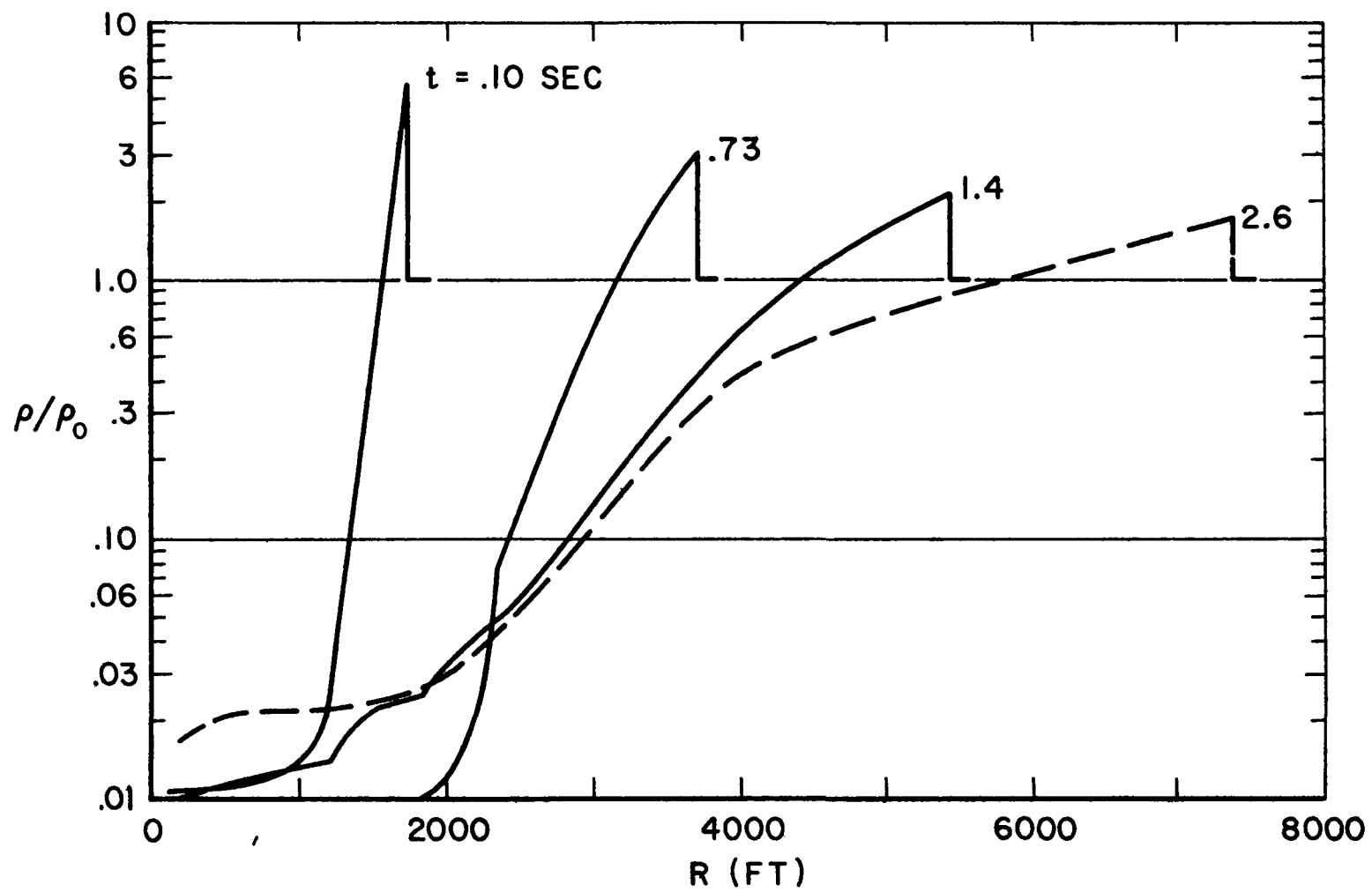


Fig. 27

P-1951  
3-31-60  
63

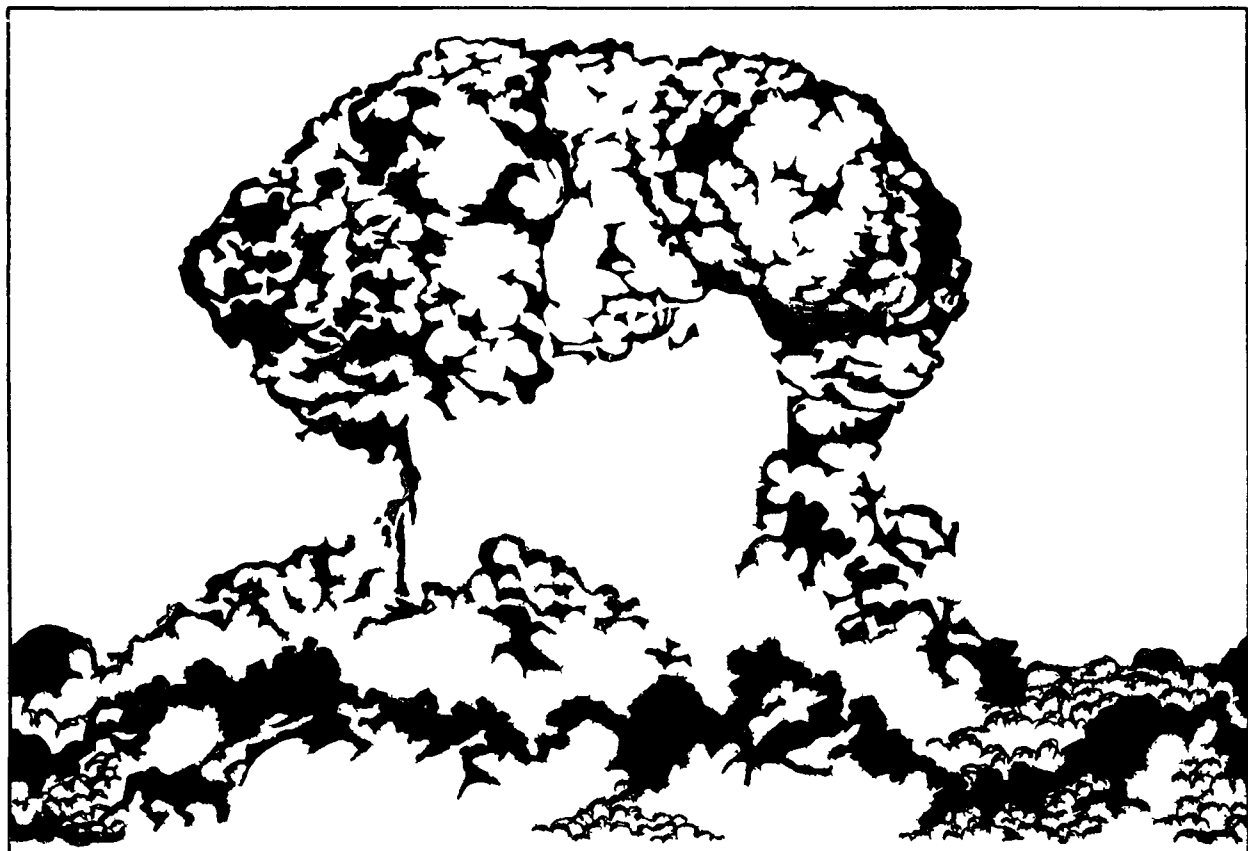


Fig. 28

BIBLIOGRAPHY - NUCLEAR RADIATION

1. Glasstone, Samuel (ed.), Effects of Nuclear Weapons, U.S. Department of Defense, Atomic Energy Commission, June 1952.
2. Nuclear Radiation Panel, Space Technology Laboratories, Inc., Nuclear Radiation Criteria for Hardened ICBM Systems, STL/TR-59-0000-00735, December 1959 (Secret).
3. Kinch, J. W., et al., Neutron Flux From Large-Yield Bursts, AFSWP ITR 1622-1, Operation Hardtack, August 22, 1958 (Secret-RD).
4. Malik, J., Summary of Gamma Radiation From Atomic Weapons, Los Alamos Scientific Laboratory, LA 1620, January 1954 (Secret-RD).
5. Etherington, H. (ed.), Nuclear Engineering Handbook, McGraw-Hill, New York, 1958.
6. Spencer, L. V. and J. C. Lamkin, Slant Penetration of Gamma Rays: Mixed Radiation Sources, National Bureau of Standards, NBS Report 6322, February 1959.
7. Basley, J. W., Comparison of Neutron Damage in Germanium and Silicon Transistors, Transactions of the IRE-Wescon, Part 3, 1958.
8. Bohan, W. A., J. D. Maxey and R. P. Pecoraro, Some Effects of Pulse Irradiation on Semiconductor Devices, IBM, March 1959.
9. Messenger, G. C. and J. P. Spratt, The Effects of Neutron Irradiation on Germanium and Silicon, Transactions of the IRE, June 1958.
10. The Effect of Nuclear Radiation on Transistors, The Radiation Effects Information Center, Batelle Memorial Institute, Tech. Memo No. 5.
11. Keister, G. L. and H. V. Stewart, "The Effects of Nuclear Radiation on Selected Semiconductor Devices," Proceedings of the IRE, Vol. 45, No. 7, p. 931, July 1957.
12. Elder, G. E., Effects of Nuclear Detonations on Nike Hercules, ITR 1439, Operation Plumbob, March 1958 (Confidential).

BIBLIOGRAPHY - AIR BLAST AND FIREBALL

1. Glasstone, Samuel (ed.), Effects of Nuclear Weapons, U.S. Department of Defense, Atomic Energy Commission, June 1952.
2. Capabilities of Atomic Weapons, Armed Forces Special Weapons Project, TM 23-200, November 1957.
3. Brode, H. L., Theoretical Description of the Blast and Fireball for a Sea Level Megaton Explosion, The RAND Corporation, Research Memorandum RM-2248, September 1959 (Secret-FRD).
4. O'Sullivan, John J. (ed.), Proceedings of the Second Protective Construction Symposium, Vols. I and II, The RAND Corporation Report R-341, March 24, 25, 26, 1959.
5. Brode, H. L., The Blast Wave in Air Resulting From a High Temperature, High Pressure Sphere of Air, The RAND Corporation, Research Memorandum RM-1825-AEC, December 3, 1956.
6. Brode, H. L., Space Plots of Pressure, Density and Particle Velocity for the Blast Wave From a Point Source in Air, The RAND Corporation, Research Memorandum RM-1913-AEC, June 3, 1957;  
and  
Brode, H. L., Point Source Explosion in Air, The RAND Corporation, Research Memorandum RM-1824-AEC, December 3, 1956.
7. Brode, H. L., Reflection Factors for Normally Reflected Shocks in Air, The RAND Corporation, Research Memorandum RM-2211, July 14, 1958.
8. Brode, H. L., Nuclear Weapons Phenomena Pertinent to Protective Design, The RAND Corporation, Research Memorandum RM-1938, July 19, 1957 (Secret-RD).
9. Moulton, J. F., Jr., Nuclear Weapons Blast Phenomena, U.S. Naval Ordnance Laboratories and Defense Atomic Support Agency, AFSWP 1048 and 1095 or NAVORD 5721 and 6085, July 1957 and 1958.

BIBLIOGRAPHY - GROUND SHOCK

1. O'Sullivan, John J. (ed.), Proceedings of the Second Protective Construction Symposium, Vols. I and II, The RAND Corporation, Report R-341, March 24, 25, 26, 1959.
2. Glasstone, Samuel (ed.), Effects of Nuclear Weapons, U.S. Department of Defense, Atomic Energy Commission, June 1952.
3. Sauer, Fred M., Ground Motion Produced by Above-Ground Nuclear Explosions, Air Force Special Weapons Center, AFSWC-TN-59-71 (Secret-FRD).
4. Barton, M. V., Ground Shock Aspects of the Hard Base Story, Space Technology Laboratories, STL/TN-60-0000-09013 (Confidential).
5. Merritt, J. L. and N. M. Newmark, Design of Underground Structures to Resist Nuclear Blast, Vol. 2, University of Illinois and Office of Engineers, Final Report DA-49-129-Eng-312, April 1958.